

# Average-Interpolating Wavelet Bases on Irregular Meshes on the Interval

*Jo Simoens  
Stefan Vandewalle*

*Report TW 310, August 2000*



Katholieke Universiteit Leuven  
Department of Computer Science  
Celestijnenlaan 200A – B-3001 Heverlee (Belgium)

# Average-Interpolating Wavelet Bases on Irregular Meshes on the Interval

*Jo Simoens*  
*Stefan Vandewalle*

*Report TW 310, August 2000*

Department of Computer Science, K.U.Leuven

## **Abstract**

The stabilized two-step construction of wavelet bases is applied to the one-dimensional case of irregular meshes on the interval. The method yields biorthogonal bases in which the wavelets on both the primal and the dual side have a chosen number of vanishing moments and have local support. The primal scaling functions are average-interpolating by construction. Uniform  $\mathbf{L}_2$ -stability is shown under a mild restriction on the irregularity of the mesh.

Numerical results show that the wavelet bases are well-conditioned, having approximately the same condition numbers as wavelet bases obtained by full semiorthogonalization, while the average support is only slightly larger than in the unstabilized construction.

**Keywords :** multiresolution analysis on the interval, irregular meshes, nonstationary or second-generation wavelets, lifting scheme, stability.

**AMS(MOS) Classification :** 42C15, 42C40, 65T60.

# Average-Interpolating Wavelet Bases on Irregular Meshes on the Interval

Jo Simoens                      Stefan Vandewalle

Department of Computer Science,  
Katholieke Universiteit Leuven, Belgium

## Abstract

The stabilized two-step construction of wavelet bases is applied to the one-dimensional case of irregular meshes on the interval. The method yields biorthogonal bases in which the wavelets on both the primal and the dual side have a chosen number of vanishing moments and have local support. The primal scaling functions are average-interpolating by construction. Uniform  $\mathbf{L}_2$ -stability is shown under a mild restriction on the irregularity of the mesh.

Numerical results show that the wavelet bases are well-conditioned, having approximately the same condition numbers as wavelet bases obtained by full semiorthogonalization, while the average support is only slightly larger than in the unstabilized construction.

## 1 Introduction

### 1.1 Motivation

In several applications including signal processing, data are given on some fixed mesh. Finding a multiscale representation then means that coarser (and possibly also finer) meshes need to be constructed which together with the given mesh form a mesh hierarchy called a multilevel mesh.

We consider multilevel meshes that are nested and dyadically refined, i.e., where two successive finer-level intervals make up a coarser-level interval. The multilevel mesh is *regular* if all single-level meshes are regular, meaning that all intervals at a given mesh level have equal length. It is *semi-regular* if it can be derived from an arbitrary coarsest-level mesh by regular dyadic refinement, splitting each interval into two congruent parts. In the most general case the nested multilevel mesh is *irregular*.

Even when the given fine-level mesh is regular, the dyadic multilevel mesh will be irregular unless the number of intervals in the fine-level mesh is a power of two. This makes irregular refinement the natural framework when a fine-level mesh is given.

In the classical, *stationary* setting, all scaling functions and all wavelets are translates and dilates of a single father c.q. mother function. Wavelet bases on regular multilevel meshes on the interval can be derived from stationary wavelet bases by an adaptation near the boundary of the interval as in, e.g., [5] and [8]. This is not possible in the irregular case. We will need to deal with nonstationary wavelet bases.

Moreover, applications such as compression and denoising in a wavelet basis impose certain properties on suitable bases. Firstly, these applications require equivalence of the  $\mathbf{L}_2$ -norm of

a signal  $f = \sum_j \sum_m c_{jm} \psi_{jm}$  and the  $\ell_2$ -norm of the sequence of its wavelet coefficients  $c$ ,

$$m \|c\|_{\ell_2} \leq \|f\|_{\mathbf{L}_2} \leq M \|c\|_{\ell_2} , \quad (1.1)$$

where  $m$  and  $M$  depend only on the wavelet basis and should be close to one another. Thus the error made in the signal by discarding one coefficient is bounded from above and from below by the magnitude of the coefficient up to the constants  $M$  and  $m$ . This defines  $\mathbf{L}_2$ -*stability* of the wavelet basis: a set satisfying (1.1) is a *Riesz basis* for its linear span. A second requirement for such applications is that the forward and inverse transforms back and forth between the single-scale basis and the wavelet basis should be computationally efficient.

## 1.2 Overview and related work

Applying [18], we use a stabilized version of a construction in [21], which is a realization of the *lifting scheme*. In a (primal) *lifting step* the scaling functions  $\varphi_{jk}$  are kept and the wavelets  $\psi_{jm}$  are modified to meet some chosen requirements by adding a linear combination of scaling functions:

$$\hat{\varphi}_{jk} := \varphi_{jk} , \quad \hat{\psi}_{jm} := \psi_{jm} - \sum_k u_{jkm} \varphi_{jk} . \quad (1.2)$$

The lifting scheme is easy to implement, gives efficient algorithms, but perhaps its main attraction is its flexibility, owing to the explicit character of (1.2). This is a helpful property when dealing with irregular meshes.

Stevenson [20] constructs stable wavelet bases of small support that are semiorthogonal with respect to a discrete  $\mathbf{L}_2$ -equivalent inner product, on locally refined semi-regular meshes in one or more dimensions. The method is similar to lifting in that a simple initial wavelet basis is modified by adding a linear combination of scaling functions, with the distinction that these are fine-level scaling functions  $\varphi_{j+1,k}$  instead of coarse-level scaling functions  $\varphi_{jk}$ . The initial wavelet basis is the hierarchical basis of Yserentant [22]. In [19], the same author identifies local semiorthogonal wavelets for interpolating piecewise linear scaling functions that are stable in a range of Sobolev spaces, again on semi-regular meshes in one or more dimensions. In [9], this is generalized to biorthogonal finite element wavelets having any number of vanishing moments. In all of these constructions, however, no efficient inverse (analysis) transform is available. While for the purpose of preconditioning this is not needed, applications like compression do use the inverse transform. Dahmen *et al.* [8] build biorthogonal wavelet bases on the interval having any desired number of primal and dual vanishing moments and allowing fast forward and inverse transforms. They consider only regular multilevel meshes. The present paper deals with irregular meshes, and we also ensure the existence of fast forward and inverse transforms. In comparison to the bases constructed in [8], the resulting wavelet bases show better conditioning by several orders of magnitude.

The remainder of the paper is organized as follows. After some preliminaries, Section 3 briefly recalls the lifting scheme and applies the analysis of the two-step construction given in more general terms in [18] to the one-dimensional case of the interval. In Section 4 we emphasize the role of nonstationary subdivision in lifting. The desired stability properties of a lifting step are seen to follow from convergence properties of a nonstationary subdivision scheme. This is applied to the first step in the two-step construction in Section 5. For the simple subdivision scheme involved, some results are available. For the second step we resort

to the methods and analysis of [18]. The construction of wavelet bases on a given irregular finest-level mesh is discussed in Section 6. We justify an approach that has previously been used as an empirical approximation. Section 7 provides detailed numerical results.

## 2 Preliminaries

Consider a *multiresolution analysis* (MRA) in  $\mathbf{L}_2$ , i.e. a strictly increasing and dense sequence  $\mathcal{V} := \{V_j\}_{j \geq 0}$  of closed subspaces of  $\mathbf{L}_2$ ,

$$V_j \subset V_{j+1}, \quad j \geq 0, \quad \text{and} \quad \text{clos} \bigcup_{j=0}^{\infty} V_j = \mathbf{L}_2 .$$

Between successive spaces in  $\mathcal{V}$ , construct algebraic complements  $W_j$  so that

$$V_{j+1} = V_j \oplus W_j ,$$

where ‘ $\oplus$ ’ denotes the inner sum of disjoint linear spaces. The complement space  $W_j$  is not necessarily orthogonal to  $V_j$ . A fine-resolution space  $V_j$  can then be written as a telescopic decomposition into a coarser-resolution space and intermediate complement spaces,

$$V_j = V_0 \oplus \bigoplus_{i=0}^{j-1} W_i . \quad (2.1)$$

With the notational convention that  $W_{-1} := V_0$ , we call the sequence  $\mathcal{W} := \{W_j\}_{j \geq -1}$  a *multiscale decomposition* (MSD).

The spaces  $V_j$  and  $W_j$  are equipped with bases,

$$\begin{aligned} V_j &= \text{clos}_{\mathbf{L}_2} \text{span } \Phi_j, & \Phi_j &:= \{ \varphi_{jk} \mid k \in \mathcal{K}_j \} , \\ W_j &= \text{clos}_{\mathbf{L}_2} \text{span } \Psi_j, & \Psi_j &:= \{ \psi_{jm} \mid m \in \mathcal{M}_j \} , \end{aligned}$$

with  $\mathcal{K}_j$  and  $\mathcal{M}_j$  arbitrary index sets. On the interval we identify them with ranges of integers. We refer to any basis  $\Phi_j$  for the space  $V_j$  as a set of *scaling functions*, and any basis  $\Psi_j$  for any type of complement space  $W_j$ ,  $j \geq 0$ , is called a set of *wavelets* at level  $j$ . In what sense the basis property must be understood is made clear below.

Because of the decomposition (2.1), an element of  $V_j$  can be expressed in two ways: in single-scale form by its coordinates  $a_j$  in the single-scale basis  $\Phi_j$ , and in multiscale form by the coefficients  $c_j$  in the *wavelet* or *multiscale basis*  $\Xi_j := \Phi_0 \cup \bigcup_{i=0}^{j-1} \Psi_i$ . We enumerate the sets  $\Phi_j$  and  $\Psi_j$  in (possibly infinite) row vectors denoted by the same symbols, and use column vectors for the coordinates  $a_j = [a_{jk}]_{k \in \mathcal{K}_j}$  and  $c_j = [a_0^T \quad b_0^T \quad \dots \quad b_{j-1}^T]^T$  (in Mallat ordering). To simplify the notation, we also define  $b_{-1} := a_0$  and  $\Psi_{-1} := \Phi_0$ . Then we can write  $\Phi_j a_j = \sum_{i=-1}^{j-1} \Psi_i b_i$ .

Use of the multiscale basis is only interesting in practice if the conversion between single-scale form and multiscale form can be performed efficiently. Because of the multiresolution structure of the spaces  $V_j$  and  $W_j$ , there exist refinement coefficients  $\{h_{jlk}\}$  and  $\{g_{jlm}\}$  such that

$$\varphi_{jk} = \sum_{l \in \mathcal{K}_{j+1}} h_{jlk} \varphi_{j+1,l} , \quad \psi_{jm} = \sum_{l \in \mathcal{K}_{j+1}} g_{jlm} \varphi_{j+1,l} . \quad (2.2)$$

The refinement relations (2.2) can be written as matrix expressions

$$\Phi_j = \Phi_{j+1}H_j \quad \text{and} \quad \Psi_j = \Phi_{j+1}G_j .$$

The refinement operators  $H_j$  and  $G_j$  readily provide an expression for the *two-scale transform*

$$a_{j+1} = A_j \begin{bmatrix} a_j \\ b_j \end{bmatrix} = H_j a_j + G_j b_j , \quad A_j := [H_j \quad G_j] . \quad (2.3)$$

The *multiscale transform*, converting from multiscale form to single-scale form, is then found by concatenating successive two-scale transforms and can be written as the application of

$$T_j := A_{j-1} \begin{bmatrix} T_{j-1} & 0 \\ 0 & I \end{bmatrix} , \quad T_1 := A_0 ,$$

where  $I$  is the identity operator on  $\ell_2(\mathcal{M}_{j-1})$ . If the spaces  $V_j$  are finite-dimensional, we may expand  $T_j$  into an  $n_j \times n_j$  matrix, where  $n_j$  is the dimension of  $V_j$ .

The inverse transform can be written in a similar fashion provided that there exist bases  $\tilde{\Phi}_j$  and  $\tilde{\Psi}_j$  that are *biorthogonal* to  $\Phi_j$  and  $\Psi_j$ , i.e.,

$$\begin{aligned} \langle \varphi_{jk}, \tilde{\varphi}_{jk'} \rangle &= \delta_{kk'} , & \langle \varphi_{jk}, \tilde{\psi}_{jm'} \rangle &= 0 , \\ \langle \psi_{jm}, \tilde{\varphi}_{jk'} \rangle &= 0 , & \langle \psi_{jm}, \tilde{\psi}_{jm'} \rangle &= \delta_{mm'} , \end{aligned} \quad (2.4)$$

where  $\delta_{kk'}$  is the Kronecker symbol. The spaces spanned by  $\tilde{\Phi}_j$  and  $\tilde{\Psi}_j$  form a second MSD  $\tilde{\mathcal{W}}$ . One then has that  $W_j \perp \tilde{V}_j$  and  $V_j \perp \tilde{W}_j$ . By convention  $\mathcal{W}$  is called the *primal* and  $\tilde{\mathcal{W}}$  is called the *dual* MSD. Assuming that such a dual MSD exists, the dual refinement operators  $\tilde{H}_j$  and  $\tilde{G}_j$  are defined analogously. Filling in the refinement relations in (2.4) gives

$$\begin{aligned} \tilde{H}_j^* H_j &= I , & \tilde{G}_j^* H_j &= 0 , \\ \tilde{H}_j^* G_j &= 0 , & \tilde{G}_j^* G_j &= I , \end{aligned}$$

which says that the inverse of the primal two-scale transform matrix  $A_j$  is given by the hermitian conjugate  $\tilde{A}_j^*$  of the dual two-scale transform matrix. Hence the inverse two-scale transform is found as

$$a_j = \tilde{H}_j^* a_{j+1} , \quad b_j = \tilde{G}_j^* a_{j+1} .$$

The inverse multiscale transform  $T_j^{-1}$  is expressed in terms of the dual two-scale transforms  $\tilde{A}_j$  as

$$T_j^{-1} := \begin{bmatrix} T_{j-1}^{-1} & 0 \\ 0 & I \end{bmatrix} \tilde{A}_{j-1}^* , \quad T_1^{-1} := \tilde{A}_0^*$$

or  $T_j^{-1} = \tilde{T}_j^*$ .

Efficiency of the forward and inverse multiscale transforms depends strongly on the matrices  $A_j$  and  $\tilde{A}_j$  being sparse. This is a property of the bases involved, as we shall see now.

Let the mesh at level  $j$  be represented by the partitioning  $\mathcal{I}_j := \{ I_{jk} \mid k \in \mathcal{K}_j \}$ . Since our meshes are one-dimensional, we identify the index set  $\mathcal{K}_j$  with a range of integers, numbering

the intervals from left to right. Since the mesh refinement is binary, every two successive fine-level intervals  $I_{j+1,l}$  and  $I_{j+1,l+1}$  with  $I_{j+1,l} \cup I_{j+1,l+1} = I_{jk}$  are associated with the same coarse-level interval  $I_{jk}$ . We can split  $\mathcal{K}_{j+1}$  in two sets, assigning  $I_{j+1,l}$  to a set of ‘even’ indices  $\mathcal{K}_{j+1}^0$  and  $I_{j+1,l+1}$  to a set of ‘odd’ indices  $\mathcal{K}_{j+1}^1$ , and correspondingly write

$$a_{j+1}^0 = H_j^0 a_j + G_j^0 b_j, \quad a_{j+1}^1 = H_j^1 a_j + G_j^1 b_j$$

and

$$a_j = (\tilde{H}_j^0)^* a_{j+1}^0 + (\tilde{H}_j^1)^* a_{j+1}^1, \quad b_j = (\tilde{G}_j^0)^* a_{j+1}^0 + (\tilde{G}_j^1)^* a_{j+1}^1.$$

This allows us to define an appropriate notion of *bandwidth* for the non-square matrix  $H_j$  as the maximum bandwidth of  $H_j^0$  and  $H_j^1$ . The bandwidth of  $G_j$  and of the dual refinement matrices is defined analogously.

We can then define locality as follows.

**Definition 2.1.** *The hierarchy of bases  $\{\Phi_j\}$  is local if the bandwidth of  $H_j$  is bounded uniformly in  $j$ . The collection of wavelet bases  $\{\Psi_j\}$  is local if the bandwidth of  $G_j$  is bounded uniformly in  $j$  and  $\{\Phi_j\}$  is local.*

If the primal bases are local, the cost of the transform  $T_j$  is linear in  $n_j$ . If both the primal and the dual bases are local, then both the forward and the inverse multiscale transforms  $T_j$  and  $T_j^{-1}$  have linear complexity. Hence in applications which require both  $T_j$  and  $T_j^{-1}$ , locality of the primal and the dual bases is desirable.

Another desirable property of the multiscale transforms  $T_j$  is that they should be well-conditioned. In particular, the condition number of  $T_j$  should be bounded independently of the number of levels  $j$ . We repeat some essential results [6, 18].

**Definition 2.2.** *A sequence of single-scale Riesz bases  $\Phi_j$  for  $V_j$  is uniformly stable if*

$$m \|a_j\|_{\ell_2} \leq \left\| \sum_{k \in \mathcal{K}_j} a_{jk} \varphi_{jk} \right\|_{\mathbf{L}_2} \leq M \|a_j\|_{\ell_2} \quad (2.5)$$

with  $0 < m, M < \infty$  independent of  $j$ . For convenience of notation, an expression like (2.5) will be written more concisely as  $\|a_j\|_{\ell_2} \lesssim \|v_j\|_{\mathbf{L}_2} \lesssim \|a_j\|_{\ell_2}$  or even  $\|v_j\|_{\mathbf{L}_2} \sim \|a_j\|_{\ell_2}$ , with  $v_j = \sum_k a_{jk} \varphi_{jk}$ .

**Theorem 2.3.** *In a MSD of  $\mathbf{L}_2$ , assume that  $\Phi_j$  are uniformly stable bases for  $V_j$ . Then the following are equivalent:*

- (i) *the multiscale transforms  $T_j$  have uniformly bounded condition numbers*
- (ii) *the multiscale basis  $\Xi_\infty := \bigcup_{j=-1}^\infty \Psi_j$  is a Riesz basis for  $\mathbf{L}_2$ .*

**Theorem 2.4.** *The multiscale basis  $\Xi_\infty$  in a MSD  $\mathcal{W}$  of  $\mathbf{L}_2$  is a Riesz basis for  $\mathbf{L}_2$  if and only if*

- (i) *the single-scale bases  $\Psi_j$  are uniformly stable bases for  $W_j$ , and*
- (ii)  *$\mathcal{W}$  is a stable MSD, i.e.,*

$$\forall v = \sum_{j=-1}^\infty w_j \in \mathbf{L}_2, \quad w_j \in W_j \quad : \quad \|v\|_{\mathbf{L}_2}^2 \sim \sum_{j=-1}^\infty \|w_j\|_{\mathbf{L}_2}^2.$$

The usual way to ensure stability of the MSD [6, 7] involves the *order* of the MRA and the number of *vanishing moments* of the wavelets.

When dealing with MRAs on possibly bounded domains, we find it convenient to use a slightly modified definition of the order of a MRA, which coincides with the usual definition in the stationary case. The reasons for this will be made clear in Section 5.1.

**Definition 2.5.** *The (polynomial) order of a nonstationary univariate MRA is given by*

$$\tilde{N} := \max\{n \mid \exists j_0 \text{ such that } \forall j \geq j_0 : \Pi_n \subset V_j \text{ on every bounded subdomain}\},$$

where  $\Pi_n$  is the space of polynomials of degree at most  $n - 1$ .

**Definition 2.6.** *The primal wavelets are said to have  $N$  vanishing moments if  $W_j$  is orthogonal to  $\Pi_N$  for  $j \geq j_0$ .*

The number of vanishing moments of the dual wavelets is of course defined analogously. One has that  $\Pi_N$  is orthogonal to  $W_j$  for all  $j \geq j_0$  if and only if  $\Pi_N \subseteq \tilde{V}_{j_0}$ . Hence the quantities  $N$  and  $\tilde{N}$  are dual to each other in that the number of primal vanishing moments  $N$  equals the order of the dual MRA and vice versa.

Finally, a necessary condition for stability of the MSD in Theorem 2.4 is given by uniform complement stability.

**Definition 2.7.** *Given  $V_{j+1} = V_j \oplus W_j$ , define*

$$\alpha_j := \sup_{\substack{v \in V_j, w \in W_j \\ v, w \neq 0}} \left| \left\langle \frac{v}{\|v\|}, \frac{w}{\|w\|} \right\rangle \right|.$$

Then  $W_j$  is a stable complement of  $V_j$  if  $\alpha_j < 1$ .

The spaces  $W_j$  in a MSD are uniformly stable complements if  $\alpha_j$  are uniformly bounded away from unity.

### 3 The Lifting Scheme

After these preliminary remarks, we recall the construction mechanism of the wavelet bases we consider, which is the lifting scheme [1, 21].

#### 3.1 Principle

A lifting step consists in the following operation. Let  $A_j = [H_j \ G_j]$  and  $\tilde{A}_j = [\tilde{H}_j \ \tilde{G}_j]$  be two-scale transform matrices from a biorthogonal pair of MSDs. A new pair of biorthogonal two-scale transform matrices are given by

$$\hat{A}_j := [\hat{H}_j \ \hat{G}_j] := [H_j \ G_j] \begin{bmatrix} I & -U_j \\ 0 & I \end{bmatrix} \text{ and } \hat{\tilde{A}}_j := [\hat{\tilde{H}}_j \ \hat{\tilde{G}}_j] := [\tilde{H}_j \ \tilde{G}_j] \begin{bmatrix} I & 0 \\ U_j^* & I \end{bmatrix}. \quad (3.1)$$

Of course, the roles of both biorthogonal MSDs in (3.1) can be interchanged. This yields the matrices

$$\hat{A}_j := [\hat{H}_j \ \hat{G}_j] := [H_j \ G_j] \begin{bmatrix} I & 0 \\ P_j & I \end{bmatrix} \text{ and } \hat{\tilde{A}}_j := [\hat{\tilde{H}}_j \ \hat{\tilde{G}}_j] := [\tilde{H}_j \ \tilde{G}_j] \begin{bmatrix} I & -P_j^* \\ 0 & I \end{bmatrix}. \quad (3.2)$$

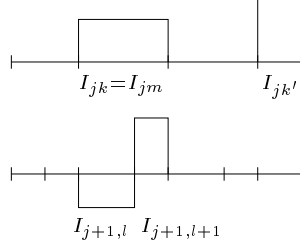


Figure 1: Two scaling functions and one wavelet in the Haar MSD on irregular meshes on the interval. Above, the mesh at level  $j$  is drawn, and below, the next finer mesh at level  $j + 1$ . Unlike the interval  $I_{jk'}$ , the interval  $I_{jk}$  is split in two subintervals at level  $j + 1$ , so besides a scaling function there is also a wavelet associated with it.

The operations (3.1) and (3.2) are known as *primal lifting* and *dual lifting*, respectively.

If  $A_j$  and  $\tilde{A}_j$  correspond to a pair of biorthogonal MSDs, then after primal lifting the primal MRA  $\mathcal{V}$  has been left unchanged. The new bases  $\hat{\Phi}_j$  and  $\hat{\Psi}_j$  are related to the old ones by  $\hat{\Phi}_j = \Phi_j$  and  $\hat{\Psi}_j = \Psi_j - \Phi_j U_j$ . This allows to easily build a new  $\hat{\Psi}_j$  out of  $\Psi_j$  and  $\Phi_j$ . One may start with a simple biorthogonal MSD and then adapt it so as to obtain certain desirable properties.

### 3.2 Two-Step Construction

The construction which we will use comprises two consecutive lifting steps, and is a simple case of what is called a *cakewalk* construction in [21]. The starting point is a trivial orthogonal MSD with orthogonal two-scale transform matrices  $[\check{H}_j \ \check{G}_j]$ . This will be the Haar MSD, spanned by the normalized characteristic functions

$$\check{\varphi}_{jk} := |I_{jk}|^{-\frac{1}{2}} \chi(I_{jk})$$

and the Haar wavelets

$$\check{\psi}_{jm} := |I_{jm}|^{-\frac{1}{2}} \left( \sqrt{\frac{|I_{j+1,l}|}{|I_{j+1,l+1}|}} \chi(I_{j+1,l+1}) - \sqrt{\frac{|I_{j+1,l+1}|}{|I_{j+1,l}|}} \chi(I_{j+1,l}) \right),$$

where  $I_{j+1,l} \cup I_{j+1,l+1} = I_{jm}$  as in Figure 1, and where  $|I_{jk}|$  denotes the length of the interval  $I_{jk}$ . Scaling functions and wavelets at level  $j$  are conveniently indexed by associating them each to an interval in the mesh  $\mathcal{I}_j$ , so that  $\mathcal{M}_j \subseteq \mathcal{K}_j$ . The sets  $\check{\Phi}_j := \{\check{\varphi}_{jk}\}$  and  $\check{\Psi}_j := \{\check{\psi}_{jm}\}$  are orthonormal bases for their closed linear spans  $\check{V}_j$  and  $\check{W}_j$ , and the MSD  $\{\check{W}_j\}$  is orthogonal.

Starting from the orthogonal MSD, we first apply a dual lifting step — or *prediction* step — to obtain a primal MSD of the desired order. In a second step — the *update* step — we use primal lifting to construct wavelets which additionally possess any number of vanishing moments that does not exceed the order. The terms *update* and *prediction* are due to an interpretation [12] of the effect of both operations. Both lifting steps are designed so as to maintain uniform stability and locality of the primal and dual bases.

This approach differs from that followed by Dahmen *et al.* in [8]. There the authors start out with a stationary biorthogonal pair of MRAs from the Cohen–Daubechies–Feauveau

family [4], both of which are then separately adapted to the interval in such a way that polynomial reproduction properties and uniform single-scale stability remain satisfied. This loses biorthogonality near the boundary, so that the bases need to be re-biorthogonalized afterwards. Finally locally supported bases are identified for the primal and dual complement spaces corresponding to the pair of biorthogonal MRAs. In contrast, we immediately obtain a pair of biorthogonal MRAs with bases that are intrinsically fitted to the interval and hence do not need any adaptation near the boundary.

Figure 2 shows plots of some basis functions at each phase in the two-step construction: (a) the orthonormal bases in the initial Haar MSD; (b,c) the primal and dual scaling functions and wavelets after a prediction step to three and seven dual vanishing moments, respectively; and (d,e) the primal and dual scaling functions and wavelets after an update step from the bases in (b) and in (c) to three and to seven primal vanishing moments, respectively.

Both consecutive steps are reflected in the multiscale transform. The two-scale transform reads

$$a_{j+1} = \begin{bmatrix} \check{H}_j & \check{G}_j \end{bmatrix} \begin{bmatrix} I & 0 \\ \check{P}_j & I \end{bmatrix} \begin{bmatrix} I & -U_j \\ 0 & I \end{bmatrix} \begin{bmatrix} a_j \\ b_j \end{bmatrix}.$$

Direct implementation in factored form leads to efficient algorithms. Often it takes significantly less operations to apply the multiscale transform in factored form than to assemble the lifted refinement matrices and multiply these with the vectors of coefficients [12].

Finally, since both the original multiscale transform and the individual lifting steps are trivially inverted, the inverse transform has a simple expression,

$$\begin{bmatrix} a_j \\ b_j \end{bmatrix} = \begin{bmatrix} I & U_j \\ 0 & I \end{bmatrix} \begin{bmatrix} I & 0 \\ -\check{P}_j & I \end{bmatrix} \begin{bmatrix} \check{H}_j^* \\ \check{G}_j^* \end{bmatrix} a_{j+1},$$

and is of the same complexity as the forward transform.

### 3.3 Stability Properties

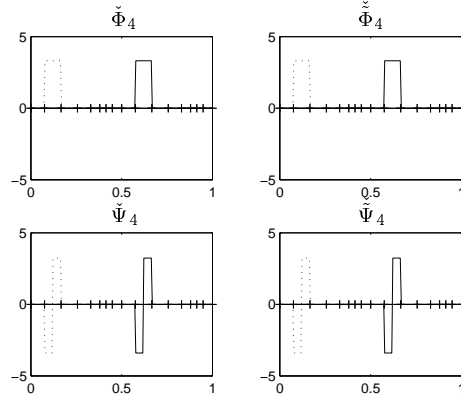
The lifting scheme also has nice stability properties, fitting in the more general theory of [1]. As it is said in the following theorem, a lifting step preserves complement stability and stability of the single-scale bases under a simple condition on the matrices  $\check{P}_j$  in (3.2). An analogous result evidently holds true on the dual side.

**Theorem 3.1 ([18]).** *Let  $\check{W}$  and  $\check{\check{W}}$ , with bases  $\check{\Phi}_j, \check{\Psi}_j$  and  $\check{\check{\Phi}}_j, \check{\check{\Psi}}_j$ , be a pair of biorthogonal MSDs. Assume that the bases  $\check{\Phi}_j$  and  $\check{\Psi}_j$  are uniformly stable and that  $\check{W}_j$  are uniformly stable complements, and use the same assumptions on the dual MSD  $\check{\check{W}}$ .*

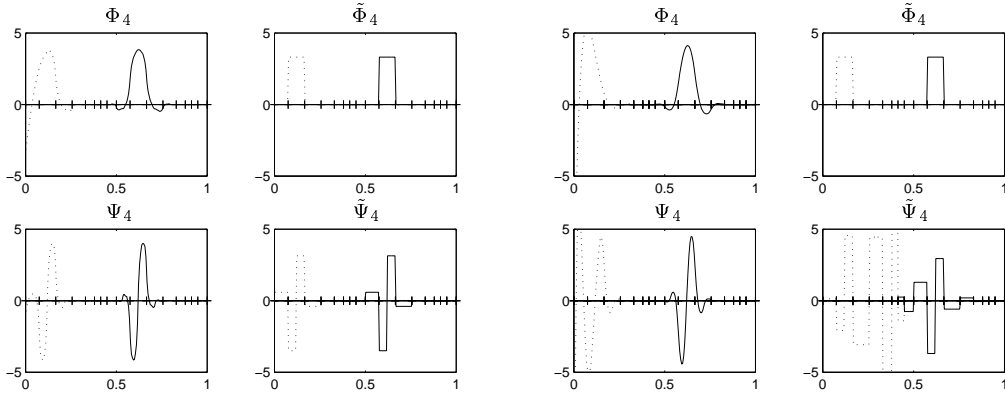
*With  $\check{H}_j, \check{G}_j$  denoting the refinement matrices in  $\check{W}$  and  $\check{\check{H}}_j, \check{\check{G}}_j$  the refinement matrices in  $\check{\check{W}}$ , the new dual refinement matrices after dual lifting,  $\check{\check{H}}_j = \check{H}_j$  and  $\check{\check{G}}_j$  as defined in (3.2), determine a new MSD  $\check{W}$ .*

*If the prediction matrices  $\check{P}_j$  in (3.2) are uniformly bounded, then the following holds:*

- (i) *The lifted bases  $\check{\check{\Phi}}_j := \check{\Phi}_j$  and  $\check{\check{\Psi}}_j := \check{\check{\Phi}}_{j+1}\check{G}_j$  are uniformly stable, and the spaces  $\check{W}_j := \text{clos}_{\mathbf{L}_2} \text{span } \check{\Psi}_j$  are uniformly stable complements.*
- (ii) *If, in addition, the lifted primal refinement matrices  $H_j$ , as defined in (3.2), determine sets of scaling functions  $\Phi_j$  that are uniformly stable then also  $\Psi_j := \Phi_{j+1}G_j$  are uniformly stable, and  $W_j := \text{clos}_{\mathbf{L}_2} \text{span } \Psi_j$  are uniformly stable complements.*

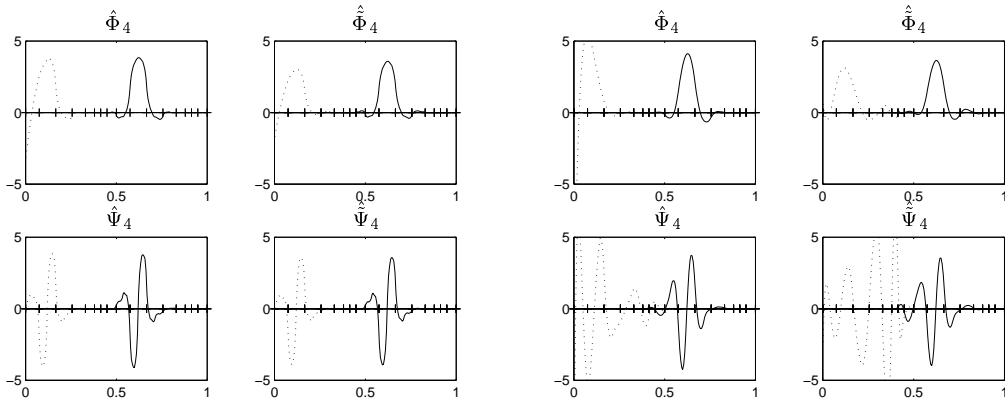


(a)  $N = \tilde{N} = 1$



(b)  $N = 1, \tilde{N} = 3$

(c)  $N = 1, \tilde{N} = 7$



(d)  $N = \tilde{N} = 3$

(e)  $N = \tilde{N} = 7$

Figure 2: Some basis functions at each phase in the two-step construction. (a) initial orthonormal bases  $\check{\Phi}_j = \check{\Phi}_j, \check{\Psi}_j = \check{\Psi}_j$ ; (b,c) bases  $\Phi_j, \tilde{\Phi}_j = \check{\Phi}_j, \Psi_j, \tilde{\Psi}_j$  after the prediction step; (d,e) bases  $\hat{\Phi}_j = \Phi_j, \hat{\Phi}_j, \hat{\Psi}_j, \hat{\Psi}_j$  after the update step.

Note that for assertion (ii) one has the additional requirement that stable sets of scaling functions exist satisfying the refinement relations with the new refinement operators  $H_j$ . This is not guaranteed. We will see that this requirement reduces to a convergence property of the subdivision scheme defined by the operators  $H_j$ , and that also uniform stability of the new bases of scaling functions follows from simple conditions on this subdivision scheme.

## 4 Multiresolution Analyses from Nonstationary Subdivision

### 4.1 Nonstationary Subdivision Schemes and Scaling Functions

Subdivision schemes are most often considered in  $\ell_\infty$  and  $\mathbf{L}_\infty$ . In order to stress the close relation with the material in the rest of this paper and to avoid renormalization of basis functions, we restate the basics of nonstationary subdivision in  $\ell_2$  and  $\mathbf{L}_2$ .

**Definition 4.1.** *A (nonstationary) subdivision scheme is a sequence of linear operators*

$$H_j : \ell_2(\mathcal{K}_j) \rightarrow \ell_2(\mathcal{K}_{j+1}) .$$

*Starting from a given sequence  $a_j \in \ell_2(\mathcal{K}_j)$ , subdivision computes a sequence  $a_{j+1} = H_j a_j$  on the next finer grid, and so on. With each iterate  $a_J, J \geq j$ , we associate a piecewise constant function*

$$\mathcal{S}_j^J(a_j) := \sum_{k \in \mathcal{K}_J} a_{Jk} \frac{\chi(I_{Jk})}{|I_{Jk}|^{\frac{1}{2}}} . \quad (4.1)$$

*A subdivision scheme is convergent if for all  $j$  and all  $a_j \in \ell_2(\mathcal{K}_j)$ , subdivision converges to a function  $\mathcal{S}_j^\infty(a_j) \in \mathbf{L}_2$ , i.e.*

$$\mathcal{S}_j^J(a_j) \rightarrow \mathcal{S}_j^\infty(a_j) \quad (4.2)$$

*in the  $\mathbf{L}_2$ -norm.*

When considered in these spaces, subdivision operators and refinement operators are the same objects. We will choose the term according to the context but always use the symbol  $H_j$ .

A convergent subdivision scheme defines basis functions spanning a sequence of nested spaces. Indeed, by linearity a bounded operator  $\mathcal{S}_j^\infty$  in a convergent subdivision scheme defines functions  $\varphi_{jk}$  such that

$$\mathcal{S}_j^\infty(a_j) = \sum_{k \in \mathcal{K}_j} a_{jk} \varphi_{jk} \quad \text{with} \quad \varphi_{jk} := \mathcal{S}_j^\infty(e_{j;k}), \quad e_{j;k} := \{\delta_{kk'}\}_{k' \in \mathcal{K}_j} .$$

An operator  $\ell_2(\mathcal{K}_j) \rightarrow \mathbf{L}_2 : a_j \mapsto \sum_{k \in \mathcal{K}_j} a_{jk} \xi_{jk}$  is usually called the *frame operator* of the set  $\{\xi_{jk}\}$ . So  $\mathcal{S}_j^\infty$  is the frame operator of  $\Phi_j := \{\varphi_{jk} \mid k \in \mathcal{K}_j\}$ . The sets  $\Phi_j$  span a sequence of nested spaces  $\mathcal{V} = \{V_j\}$ . If  $\mathcal{V}$  is dense, it is a MRA, with the functions  $\varphi_{jk}$  as scaling functions. This is why we use the same notation  $\varphi_{jk}$  as for scaling functions.

Also here, we focus our attention on *local* subdivision schemes.

**Definition 4.2.** *A subdivision scheme  $\{H_j\}$  is local if the bandwidth of  $H_j$  is uniformly bounded.*

This of course implies that the number of elements in the *mask*

$$\mathcal{L}(j, k) := \{l \in \mathcal{K}_{j+1} \mid h_{jlk} \neq 0\} \tag{4.3}$$

(the *mask size*) is bounded uniformly in  $k$  and  $j$ , corresponding to uniform boundedness of the number of nonzero elements per row of  $H_j$ . In most of the following only this number matters, but for consistency we have defined locality of a subdivision scheme to be equivalent to locality of refinement relations as introduced in Definition 2.1.

Locality has immediate consequences for the support of the scaling functions  $\varphi_{jk}$ .

**Definition 4.3.** *Following [11], we call a multilevel mesh homogeneous if*

$$\gamma := \sup_j \sup_{k, k' \text{ adjacent} \in \mathcal{K}_j} \frac{|I_{jk'}|}{|I_{jk}|} \tag{4.4}$$

*is finite.*

**Definition 4.4.** *The sets  $\Phi_j$  are locally finite if*

$$\sup_{k \in \mathcal{K}_j} \#\{k' \in \mathcal{K}_j \mid \text{supp } \varphi_{jk'} \cap \text{supp } \varphi_{jk} \neq \emptyset\} \lesssim 1 .$$

**Lemma 4.5.** *If the subdivision scheme  $\{H_j\}$  is local, and if the multilevel mesh is homogeneous, then the sets  $\Phi_j$  are locally finite and  $|\text{supp } \varphi_{jk}| \lesssim |I_{jk}|$ .*

*Proof.* By an argument completely analogous to the regular case [2, 3, 16], one finds that on a homogeneous mesh with homogeneity constant  $\gamma$ , the support of the iterates in (4.2) satisfies

$$\forall J > j : |\text{supp } \mathcal{S}_j^J(e_{j;k})| \leq |I_{jk}| \frac{\gamma^{b+1} - 1}{\gamma - 1} ,$$

with  $b$  the assumed uniform bound on the mask size in (4.3). This means that  $|\text{supp } \varphi_{jk}| \lesssim |I_{jk}|$ . Moreover, one has that

$$\text{supp } \varphi_{jk} \subset \bigcup_{i=-b}^b I_{j, k+i} ,$$

which implies local finiteness. □

Because of this bound on the diameter of the support of the limit functions  $\varphi_{jk}$ , convergence in one norm and in another norm are related. Local subdivision schemes  $\{H'_j\}$  that are convergent in the  $\mathbf{L}_\infty \leftarrow \ell_\infty$  sense are also convergent in our definition, which uses  $\mathbf{L}_2$  and  $\ell_2$ , after the scaling

$$H_j := \text{diag}[|I_{j+1, l}|^{\frac{1}{2}}] H'_j \text{diag}[|I_{j, k}|^{-\frac{1}{2}}] .$$

## 4.2 Biorthogonal Subdivision and Stability

A pair of convergent subdivision schemes with biorthogonal subdivision matrices yield scaling functions that are biorthogonal. This is easily seen to follow from biorthogonality of the iterates (4.1). The average-interpolating subdivision scheme in Section 5.1 will provide an example of biorthogonal subdivision schemes.

Furthermore, for scaling functions derived from local biorthogonal subdivision schemes, uniform boundedness is sufficient for uniform stability.

**Lemma 4.6** ([8, Lemma 2.1]). *If the sets of functions  $\Phi_j, \tilde{\Phi}_j$  are biorthogonal, uniformly  $\mathbf{L}_2$ -bounded and locally finite, then  $\Phi_j$  and  $\tilde{\Phi}_j$  are uniformly stable Riesz bases for their closed linear spans.*

*Remark 4.7.* The scaling functions  $\varphi_{jk}$  are  $\mathbf{L}_2$ -bounded uniformly in  $k$  and  $j$  if and only if the operators  $\mathcal{S}_j^\infty$  are uniformly bounded as operators from  $\ell_2(\mathcal{K}_j)$  into  $\mathbf{L}_2$ .

Often the subdivision scheme has some amount of stationarity, in that the same algorithm is used in applying  $H_j$  at all levels  $j$ , but the subdivision coefficients that make up  $H_j$  depend on the mesh. If the operators  $\mathcal{S}_j^\infty$  in Remark 4.7 are instances  $\mathcal{S}(\cdot; \{\mathcal{I}_i\}_{i>j})$  of a single general operator parameterized with the multilevel mesh, then boundedness of the general operator uniformly in the choice of the mesh is a sufficient condition for uniform boundedness of the scaling functions.

## 5 The Prediction Step

We now use the results of Section 4 in the analysis of the subdivision scheme for the new scaling functions in the prediction step. This is feasible due to the simplicity of the initial MSD. In the update step the subdivision scheme is more complex, and we refrain from a direct analysis. We instead apply the stabilized update method discussed in [18].

The subdivision schemes occurring in a prediction step from the Haar MSD belong to the class of *average-interpolating* subdivision schemes, for which the scaling functions  $\varphi_{jk}$  satisfy

$$\int_{I_{jk'}} \varphi_{jk} = |I_{jk'}|^{\frac{1}{2}} \delta_{kk'} .$$

Like in the Haar MSD, each scaling function is naturally associated to an interval in the multilevel mesh.

### 5.1 Average-Interpolating Subdivision

The average-interpolating subdivision schemes that we use were proposed by Donoho [14] in the stationary setting. The generalization to irregular meshes is trivial. Since we will need some of the details of average-interpolating subdivision below, we briefly recall the algorithm in the notation of this paper.

In average-interpolating subdivision of order  $p$ , the finer-level coefficient  $a_{j+1,l}$  is calculated from a set of  $p = 2d + 1$  consecutive coarse-level coefficients:

$$\begin{array}{ccccccc}
a_{j,k(l)-d} & \cdots & a_{j,k(l)} & \cdots & a_{j,k(l)+d} & & \\
& & \searrow & \downarrow & \swarrow & & \\
& & & a_{j+1,l} & & & 
\end{array}$$

Since scaling functions are associated to intervals, symmetry leads us to consider only odd orders. To find  $a_{j+1,l}$ , set up the polynomial  $\lambda_{j,k(l)} \in \Pi_p$  such that the averages of  $\lambda_{j,k(l)}$  over the intervals  $I_{j,k(l)+i}$  correspond to the values  $a_{j,k(l)+i}$ ,

$$\langle \lambda_{j,k}, \check{\varphi}_{j,k+i} \rangle = a_{j,k+i}, \quad -d \leq i \leq d, \quad (5.1)$$

with  $k = k(l)$ , and use its average over  $I_{j+1,l}$  as the value for  $a_{j+1,l}$ ,

$$a_{j+1,l} := \langle \lambda_{j,k(l)}, \check{\varphi}_{j+1,l} \rangle.$$

Whenever possible the associated intervals are chosen symmetrically around  $I_{j+1,l}$ , i.e.,  $I_{j,k(l)} \supset I_{j+1,l}$ . Close to the boundary this cannot be satisfied, and the coarse-level intervals have to be chosen asymmetrically around  $I_{j+1,l}$ .

It is easily checked that the above procedure does indeed give refinement matrices  $H_j$  which satisfy  $\check{H}_j^* H_j = I$ , with  $\check{H}_j$  the refinement matrices of  $\check{\Phi}_j$ .

One of the purposes of a lifting operation is to provide the new primal MRA with a certain order  $\tilde{N}$ . In terms of the subdivision scheme, this is clearly equivalent to the property that for any polynomial  $f \in \Pi_{\tilde{N}}$ , and for  $j \geq j_0$ , there is some sequence  $a_j$  which (locally) produces the polynomial  $f$ , i.e.  $S_j^\infty(a_j) = f$ . In the subdivision context the latter is referred to as the *polynomial reproduction* property of order  $\tilde{N}$ .

For  $a_{jk} = \langle f, \check{\varphi}_{jk} \rangle$  with  $f \in \Pi_p$ , the polynomial  $\lambda_{jk}$  in (5.1) coincides with  $f$  for all  $k$ . Thus average-interpolating subdivision of order  $p$  has the polynomial reproduction property of order  $\tilde{N} = p$ . At the coarsest levels in the mesh, where  $\#\mathcal{K}_j < p$ , the  $p$  coarse-level coefficients needed to perform order  $p$  average-interpolating subdivision are not available, so that the order needs to be lowered. This has no effect on the order of the MRA according to Definition 2.5. Figure 3 shows the bases for the first four levels of a MRA of order five, where the coarsest level  $V_0$  is one-dimensional. Note that the presence of a minimum level  $j_0$  in the definition of the order avoids that any MRA on a bounded domain with a one-dimensional coarsest resolution level  $V_0$  could only be of order 1, which says nothing about its approximation power.

Because of the simple form of this subdivision scheme, some properties can be derived directly. The next lemma would follow from uniform stability of the bases of scaling functions (considered in Proposition 5.4). However, it is not difficult to give a direct and constructive proof.

**Lemma 5.1.** *Let  $\mathcal{S}(\cdot; \{\mathcal{I}_j\})$  be the average-interpolating subdivision scheme of order  $p$  on a homogeneous multilevel mesh  $\{\mathcal{I}_j\}$ . Then the subdivision operators  $H_j$  are uniformly bounded, with a bound depending only on  $p$  and on the homogeneity constant of the mesh.*

*Proof.* For  $\mathcal{I}_j = \{I_{jk} \mid k \in \mathcal{K}_j\}$  and  $I_{jk} = [x_{jk}, x_{j,k+1}]$ , define  $A_{jk}(x) := \int_{x_{j,k-d}}^x \lambda_{jk}$  with  $\lambda_{jk}$  from (5.1). Being of degree  $p = 2d + 1$ , the polynomial  $A_{jk}$  is uniquely determined by the interpolation conditions

$$A_{jk}(x_{j,k+\delta}) = \sum_{i=-d}^{\delta-1} |I_{j,k+i}|^{\frac{1}{2}} a_{j,k+i}, \quad -d \leq \delta \leq d+1,$$

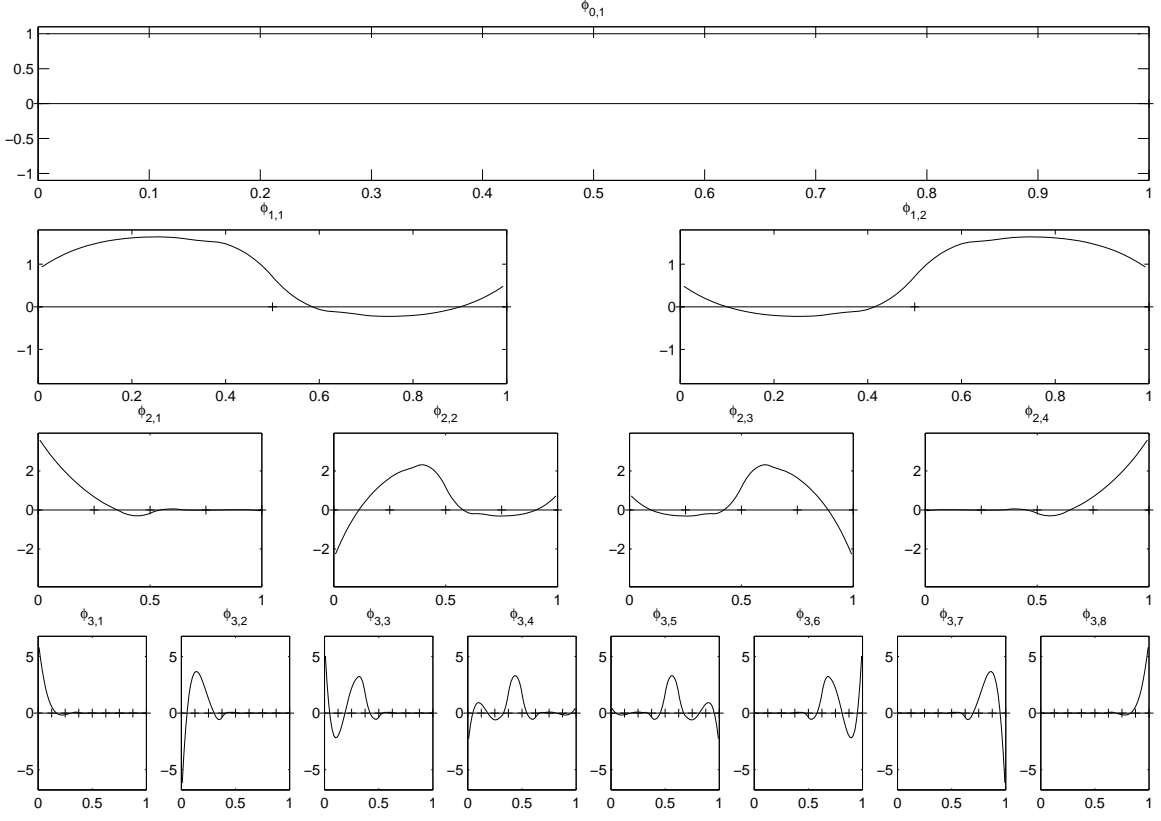


Figure 3: Single-scale basis functions for the coarsest levels in an average-interpolating MRA of order five. Constant functions are in  $V_0$ , quadratic polynomials are in  $V_2$ , and all polynomials of degree up to four are in  $V_3$ .

or

$$\Lambda_{jk} = \sum_{i=-d}^d |I_{j,k+i}|^{\frac{1}{2}} a_{j,k+i} \Lambda_{jk}^i ,$$

with  $\Lambda_{jk}^i$  such that

$$\begin{aligned} \Lambda_{jk}^i(x_{j,k-d}) &= \cdots = \Lambda_{jk}^i(x_{j,k+i}) = 0 , \\ \Lambda_{jk}^i(x_{j,k+i+1}) &= \cdots = \Lambda_{jk}^i(x_{j,k+d+1}) = 1 . \end{aligned}$$

The new coefficient  $a_{j+1,l}$  is found as

$$a_{j+1,l} = |I_{j+1,l}|^{-\frac{1}{2}} \left( \Lambda_{j,k(l)}(x_{j+1,l+1}) - \Lambda_{j,k(l)}(x_{j+1,l}) \right) ,$$

so that the subdivision coefficients  $h_{j,k(l)+i,l}$  are given by

$$h_{j,k(l)+i,l} = \sqrt{\frac{|I_{j,k(l)+i}|}{|I_{j+1,l}|}} \left( \Lambda_{j,k(l)}^i(x_{j+1,l+1}) - \Lambda_{j,k(l)}^i(x_{j+1,l}) \right) \quad (5.2)$$

for  $-d \leq i \leq d$ . The other entries in the  $l$ th row of  $H_j$  are zero. Near the boundary, the subdivision stencil is asymmetrical. This causes the maximum number of nonzero entries in a column of  $H_j$  to be  $6d + 2$ , in the  $p$ th column.

Using in (5.2) the explicit form for  $A_{jk}^i(x)$  as a sum of Lagrange polynomials,

$$A_{jk}^i(x) = \sum_{\delta=i+1}^{d+1} \prod_{\substack{\beta=-d \\ \beta \neq \delta}}^{d+1} \frac{x - x_{j,k+\beta}}{x_{j,k+\delta} - x_{j,k+\beta}}$$

we find that

$$|h_{j,k(l)+i,l}| \leq 2p(1+\gamma)^{\frac{1}{2}} \gamma^{\frac{d}{2}} \max_{\substack{-d+1 \leq \delta \leq d+1 \\ x \in I_{j,k(l)}}} \left| \prod_{\substack{\beta=-d \\ \beta \neq \delta}}^{d+1} \frac{x - x_{j,k(l)+\beta}}{x_{j,k(l)+\delta} - x_{j,k(l)+\beta}} \right|.$$

The maximum is dilation invariant and for fixed  $p$ , depends solely on the relative sizes of the intervals  $I_{j,k(l)-d}$  through  $I_{j,k(l)+d}$ , whose ratios are bounded by a function of  $\gamma$ . We conclude that the subdivision coefficients are bounded independently of  $k$  and  $j$ .

Since the matrix  $H_j$  has bandwidth independent of  $j$  and uniformly bounded elements, its 1-norm is bounded uniformly in  $j$ . For matrices with uniformly bounded bandwidth, the 1-norm and the 2-norm are equivalent uniformly in the dimensions of the matrix, so that also  $\|H\|_2$  is uniformly bounded.  $\square$

There is a useful connection with irregular Deslauriers–Dubuc *interpolating* subdivision [11, 13, 15]. A subdivision step of the sequence  $\{A_{jk}\}$  in the Deslauriers–Dubuc scheme of order  $2d$  evaluates the interpolating polynomial through the point values  $(x_{j,k(l)-d}, A_{j,k(l)-d}), \dots, (x_{j,k(l)+d+1}, A_{j,k(l)+d+1})$  at the point  $x_{j+1,l}$  to find the value  $A_{j+1,l}$  in the subdivided sequence. The subdivision scheme is evidently interpolating. The following result is an extension of [14, Lemma 2.2] to the irregular setting. It is a straightforward instance of a commutation formula for irregular subdivision [10, 11].

**Lemma 5.2.** *Let  $A_j = \{A_{jk}\}$  be iterates in the Deslauriers–Dubuc subdivision scheme of order  $p + 1$ ,  $p > 0$ , on the multilevel mesh  $\{I_{jk} = [x_{jk} \ x_{j,k+1}]\}$ , and define*

$$a_{jk} = \frac{A_{j,k+1} - A_{jk}}{\sqrt{x_{j,k+1} - x_{jk}}}. \quad (5.3)$$

*Then the sequences  $a_j = \{a_{jk}\}$  are related by the average-interpolating subdivision scheme of order  $p$  on the same mesh.*

*Proof.* We show that average-interpolating subdivision of order  $p$  applied to  $a_j$  produces the sequence  $a_{j+1}$ , preserving the relation (5.3) at the next finer level.

For any  $j$  and any  $k = k(l)$ , the polynomial  $\lambda_{jk}$  from (5.1) used in average-interpolating subdivision of the sequence  $a_j$ , can be found as the derivative of a polynomial  $\kappa_{jk}$  of degree  $p = 2d + 1$  determined by

$$\kappa_{jk}(x_{j,k+\delta}) = c + \sum_{i=-d}^{\delta-1} |I_{j,k+i}|^{\frac{1}{2}} a_{j,k+i},$$

with  $-d \leq \delta \leq d$  and  $c$  an arbitrary constant. So as long as  $A_{j,k-d}, \dots, A_{j,k+d+1}$  satisfy

$$A_{j,k+\delta+1} = A_{j,k+\delta} + |I_{j,k+\delta}|^{\frac{1}{2}} a_{j,k+\delta}, \quad -d \leq \delta \leq d,$$

the polynomial  $\lambda_{jk}$  equals the derivative of the interpolating polynomial  $\kappa_{jk}$  through the values  $(x_{j,k-d}, A_{j,k-d}), \dots, (x_{j,k+d+1}, A_{j,k+d+1})$ . Since, moreover, Deslauriers–Dubuc subdivision chooses  $k(l)$  in the same way as average-interpolating subdivision,  $\kappa_{j,k(l)}$  is precisely the interpolating polynomial used in Deslauriers–Dubuc subdivision of order  $p+1$  applied to the sequence  $A_j$ .

For any  $l \in \mathcal{K}_{j+1}$  the finer-level coefficient  $a'_{j+1,l}$  resulting from average-interpolating subdivision of  $a_j$  is found as

$$a'_{j+1,l} := \langle \lambda_{j,k(l)}, \check{\varphi}_{j+1,l} \rangle = |I_{j+1,l}|^{-\frac{1}{2}} \int_{I_{j+1,l}} \lambda_{j,k(l)}.$$

Since  $\lambda_{j,k(l)}$  equals the derivative of the polynomial  $\kappa_{j,k(l)}$  which is evaluated in Deslauriers–Dubuc subdivision of  $A_j$ , this gives

$$\begin{aligned} a'_{j+1,l} &= |I_{j+1,l}|^{-\frac{1}{2}} (\kappa_{j,k(l)}(x_{j+1,l+1}) - \kappa_{j,k(l)}(x_{j+1,l})) \\ &= |I_{j+1,l}|^{-\frac{1}{2}} (A_{j+1,l+1} - A_{j+1,l}), \end{aligned}$$

which equals  $a_{j+1,l}$ . □

The problem of convergence of the subdivision scheme on the interval can be reduced to convergence on meshes without boundary. Asymmetrical average-interpolation near the boundary corresponds to polynomial extrapolation at the starting level followed by ordinary symmetrical average-interpolation. The reasoning in [14] for regular meshes carries over to the irregular case.

Convergence of average-interpolating subdivision schemes on regular meshes is known. The resulting scaling functions are a subclass of the Cohen–Daubechies–Feauveau family [4]. Convergence on irregular meshes appeared in [11] as a side-effect in the analysis of Deslauriers–Dubuc interpolating subdivision schemes. On homogeneous irregular meshes, it has been proven only for order 1 and 3, and partial results are available for order 5.

**Proposition 5.3.** *On regular meshes or on irregular meshes with  $p < 5$ , average-interpolating subdivision of odd order  $p$  on homogeneous multilevel meshes converges and is uniformly bounded.*

*Proof.* For  $p = 1$ , the statement is trivial because all iterates are equal. The limit function is piecewise constant.

For  $p = 3$  it is shown in [11] that under the given assumptions, the first-order divided differences of iterates in Deslauriers–Dubuc subdivision

$$\sum_{k \in \mathcal{K}_J} A_{Jk}^{[1]} \chi(I_{Jk}), \quad A_{Jk}^{[1]} := \frac{A_{J,k+1} - A_{Jk}}{x_{J,k+1} - x_{Jk}}, \quad J \geq j, \quad (5.4)$$

converge in  $\mathbf{L}_\infty$ . By Lemma 5.2, the iterates in (5.4) equal  $\mathcal{S}_j^J(a_j)$  for  $A_{j,k+1} = A_{jk} + |I_{jk}|^{1/2} a_{jk}$ . For any given  $\gamma \geq 1$ , one has that the norms

$$\|\mathcal{S}_j^\infty \circ \text{diag}[|I_{jk}|^{1/2}]\|_{\mathbf{L}_\infty \leftarrow \ell_\infty} \quad (5.5)$$

are bounded uniformly in the choice of the mesh for meshes with homogeneity constant not exceeding  $\gamma$ . Hence the norms (5.5) are bounded uniformly in  $j$  and  $\|\varphi_{jk}\|_{\mathbf{L}_\infty} \lesssim |I_{jk}|^{-1/2}$ . Since by Lemma 4.5,  $|\text{supp } \varphi_{jk}| \lesssim |I_{jk}|$ , it holds that  $\|\varphi_{jk}\|_{\mathbf{L}_2} \lesssim 1$ .

For  $p > 3$ , convergence is known in the regular setting [14], both on the real line and on the interval. Here uniform boundedness is automatic. Convergence and uniform boundedness on irregular meshes could in principle be verified by a similar procedure as for  $p = 3$ , but the calculations become increasingly complicated for higher orders and have not been performed.  $\square$

There are experimental indications that similar properties hold for higher-order average-interpolating subdivision, but for now, when dealing with irregular meshes, we will need to require convergence of the subdivision scheme as an extra condition on the mesh besides homogeneity.

Using Section 4 we finally arrive at the following result.

**Proposition 5.4.** *If the multilevel mesh is homogeneous and such that average-interpolating subdivision converges and is uniformly bounded, then the subdivision scheme defines a MRA in  $\mathbf{L}_2$  with single-scale bases that are uniformly stable.*

*Proof.* We first show that the single-scale bases  $\Phi_j$  are uniformly stable. For this we can draw upon earlier lemma's. By Lemma 4.5, locality of the subdivision scheme implies local finiteness of the bases  $\Phi_j$ . These are by construction biorthogonal to the orthonormal bases of scaling functions  $\check{\Phi}_j$  of the Haar MRA. Hence, using Lemma 4.6, we conclude that  $\Phi_j$  are uniformly stable bases for their closed linear spans  $V_j$ .

The spaces  $V_j$  are nested by construction. It remains to show that  $\bigcup_{j=0}^{\infty} V_j$  is dense in  $\mathbf{L}_2$ . Let  $\check{F}_j$  and  $F_j$  denote the frame operators of  $\check{\Phi}_j$  and  $\Phi_j$ , respectively. A projection of  $v \in \mathbf{L}_2$  into  $V_j$  is given by

$$F_j \check{F}_j^* v = \sum_{k \in \mathcal{K}_j} \langle v, \check{\varphi}_{jk} \rangle \varphi_{jk} .$$

Using the triangle inequality and noting that by biorthogonality,

$$\check{F}_j \check{F}_j^* (F_j \check{F}_j^* v) = \sum_{k \in \mathcal{K}_j} \left\langle \sum_{k' \in \mathcal{K}_j} \langle v, \check{\varphi}_{jk'} \rangle \varphi_{jk'}, \check{\varphi}_{jk} \right\rangle \check{\varphi}_{jk} = \sum_{k \in \mathcal{K}_j} \langle v, \check{\varphi}_{jk} \rangle \check{\varphi}_{jk} = \check{F}_j \check{F}_j^* v ,$$

gives

$$\begin{aligned} \|v - F_j \check{F}_j^* v\|_{\mathbf{L}_2} &\leq \|v - \check{F}_j \check{F}_j^* v\|_{\mathbf{L}_2} + \|F_j \check{F}_j^* v - \check{F}_j \check{F}_j^* v\|_{\mathbf{L}_2} \\ &= \|v - \check{F}_j \check{F}_j^* v\|_{\mathbf{L}_2} + \|F_j \check{F}_j^* v - \check{F}_j \check{F}_j^* (F_j \check{F}_j^* v)\|_{\mathbf{L}_2} . \end{aligned}$$

For the Haar MRA, one has that on a homogeneous multilevel mesh, for all  $v \in \mathbf{L}_2$ , the error of the orthogonal projection  $\|v - \check{F}_j \check{F}_j^* v\|_{\mathbf{L}_2}$  goes to zero for increasing  $j$ . The same thing of course holds for the second term, which is merely the result of substituting  $F_j \check{F}_j^* v$  for  $v$ . Hence  $\bigcup_{j \geq 0} V_j$  is dense in  $\mathbf{L}_2$ , and  $\mathcal{V}$  forms a MRA.  $\square$

## 5.2 Construction by Dual Lifting

Average-interpolating subdivision can be implemented by dual lifting from the orthogonal Haar MSD. Doing so will automatically provide bases for the complement spaces in the pair of biorthogonal MSDs.

In fact, any refinement matrix  $H_j$  that is biorthogonal to some dual refinement matrix  $\check{H}_j$  in a known biorthogonal MSD can be obtained by dual lifting. If the two-scale transform matrices  $[\check{H}_j \check{G}_j]$  and  $[\check{H}_j \check{G}_j]$  are biorthogonal, then

$$H_j = [\check{H}_j \check{G}_j] \begin{bmatrix} \check{H}_j^* \\ \check{G}_j^* \end{bmatrix} H_j = [\check{H}_j \check{G}_j] \begin{bmatrix} I \\ \check{G}_j^* H_j \end{bmatrix},$$

which corresponds to a dual lifting step with the prediction operator

$$\check{P}_j = \check{G}_j^* H_j.$$

In lifting from the orthogonal Haar MSD,  $\check{H}_j = \check{H}_j$  and  $\check{G}_j = \check{G}_j$  are the Haar refinement matrices, and the coefficients for average-interpolating prediction are given by

$$\begin{aligned} \check{p}_{jmk} &= \overline{\check{g}_{jlm}} h_{jlk} + \overline{\check{g}_{j,l+1,m}} h_{j,l+1,k} \\ &= |I_{jm}|^{-\frac{1}{2}} \left( -|I_{j+1,l+1}|^{\frac{1}{2}} h_{jlk} + |I_{j+1,l}|^{\frac{1}{2}} h_{j,l+1,k} \right), \end{aligned} \quad (5.6)$$

with  $I_{jm} = I_{j+1,l} \cup I_{j+1,l+1}$ . If we show that the prediction operators are uniformly bounded, then uniform stability of the primal and dual wavelet bases and uniform complement stability follow from Theorem 3.1. This is done in the following theorem.

**Theorem 5.5.** *Let  $\check{W}$  be the orthogonal Haar MSD, with orthonormal bases  $\check{\Phi}_j$  and  $\check{\Psi}_j$ . If the mesh is homogeneous and is such that average-interpolating subdivision of order  $\check{N}$  converges and is uniformly bounded, then*

- (i) *average-interpolating dual lifting of order  $\check{N}$  defines a pair of biorthogonal MSDs in  $\mathbf{L}_2$ ,*
- (ii) *the bases  $\Phi_j, \Psi_j$  in the new primal MSD and  $\check{\Phi}_j, \check{\Psi}_j$  in the new dual MSD are local and uniformly stable, and*
- (iii) *the spaces  $W_j := \text{clos}_{\mathbf{L}_2} \text{span } \Psi_j, \check{W}_j := \text{clos}_{\mathbf{L}_2} \text{span } \check{\Psi}_j$  are uniformly stable complements.*

*Proof.* We show that the conditions for application of Theorem 3.1 are satisfied.

By Proposition 5.4 the new bases  $\check{\Phi}_j$  exist, span a MRA of  $\mathbf{L}_2$  and are uniformly stable. By construction, they are biorthogonal to  $\check{\Phi}_j$ .

Let  $\check{P}_j$  denote the matrix of prediction coefficients at the  $j$ th level, given by (5.6). Like  $H_j$ , the matrix  $\check{P}_j$  also has at most  $\check{N} = 2d + 1$  nonzero entries per row. Asymmetry in the subdivision stencil near the boundary brings the maximum number of nonzero entries per column to  $3d + 1$ , which is still independent of  $j$ . This implies locality after dual lifting. Uniform boundedness of  $\check{P}_j = \check{G}_j^* H_j$  follows from uniform boundedness of  $\check{G}_j$  and  $H_j$ , which follow from uniform stability of the bases  $\Phi_j, \check{\Phi}_j$  and  $\Psi_j$ .

Uniform stability of the bases  $\Psi_j$  and  $\check{\Psi}_j$  and uniform complement stability then follow by Theorem 3.1.  $\square$

## 6 Half Multiscale Decompositions

Before coming to numerical experiments, we comment on a practical approach to a practical problem.

As we mentioned in the introduction, often data are given on a finest-level mesh and thereby a finite-dimensional finest-level space  $V_J^J$  is fixed. This is the case when discrete data on some fixed mesh are given for processing, and one does not have access to details at finer levels or does not even care. A multilevel mesh with a finite number of levels must be built upon the given finest-level mesh by a dyadic coarsening procedure. Here we use a simple coarsening strategy: Every two successive intervals are lumped together to give a coarser-level interval, starting at the left boundary. On this multilevel mesh, we wish to construct a MSD of the given space  $V_J^J$ . Since the resulting MSD is truncated at a predetermined level  $J$ , we call it a *half multiscale decomposition*.

Also, in practice—and in the numerical examples of Section 7—subdivision will not be performed ad infinitum. When subdivision is stopped at some level  $J$ , this again gives a half MSD.

We assume that the finest-level basis is the orthonormal basis of Haar scaling functions  $\check{\Phi}_J$ . Data from  $\mathbf{L}_2$  are given as their orthogonal projection onto  $V_J^J$ . A MRA of  $V_J^J$  can then be built by running the average-interpolating subdivision scheme up to level  $J$ . This gives as scaling functions and resulting spaces

$$\varphi_{jk}^J := \mathcal{S}_j^J(e_{j;k}) \quad \text{and} \quad V_j^J := \text{clos span } \Phi_j^J .$$

If the subdivision scheme converges, then for increasing  $J$  the scaling functions  $\varphi_{jk}^J$  converge to  $\varphi_{jk} := \mathcal{S}_j^\infty(e_{j;k})$ , the scaling functions from full subdivision. This construction was already proposed in [21], and is similar in design to the ‘hybrid wavelet transforms’ introduced in [14]. Here we intend to show that it has a clear mathematical meaning allowing to draw conclusions on stability and compression properties.

Since the collections of limit scaling functions  $\Phi_j$  are biorthogonal to  $\check{\Phi}_j$ , their  $\mathbf{L}_2$ -orthogonal projection onto  $V_J^J$  satisfies

$$Q_J \varphi_{jk} = Q_J \sum_{l \in \mathcal{K}_J} a_{Jl} \varphi_{Jl} = \sum_{l \in \mathcal{K}_J} a_{Jl} \check{\varphi}_{Jl} = \varphi_{jk}^J ,$$

where  $a_J = H_{J-1} \cdots H_J e_{j;k}$ . Hence  $\Phi_j^J = Q_J \Phi_j$ , and since  $\Psi_j^J = \Phi_{j+1}^J G_j$  and for  $j < J$  obviously  $\check{\Phi}_j = Q_J \check{\Phi}_j$  and  $\check{\Psi}_j = Q_J \check{\Psi}_j$ , the constructed biorthogonal pair of half MSDs is simply the orthogonal projection of the pair of limit MSDs onto  $V_J^J = \tilde{V}_J^J$ . For the subsequent update step, the relevant spaces of polynomials are first orthogonally projected into  $V_J^J$ .

Approximation-theoretical notions such as the order of a half MSD thus make sense as properties of the underlying limit MSD. Although the spaces  $V_J^J$  (where  $J$  is regarded as variable) have poor approximation power and  $\Pi_n \not\subset V_j^J$  for  $n > 0$ , when the variable index is taken to be  $j$  one has that if the order of the limit MSD is  $\tilde{N}$  then for all  $v$  in the Sobolev space  $\mathbf{H}^{\tilde{N}}$ ,

$$\inf_{v_j^J \in V_j^J} \|Q_J v - v_j^J\|_{\mathbf{L}_2} \lesssim 2^{-\tilde{N}j} \|v\|_{\mathbf{H}^{\tilde{N}}}$$

uniformly in  $J$ , by the corresponding property of the limit MSD.

When the single-scale basis at the finest level is orthonormal, many characteristics of the bases in a finite half MSD are easy to calculate explicitly. At this point we drop the superindex  $J$  to simplify notation.

The Riesz condition number of the multiscale basis  $\Xi_J$  equals the condition number of the multiscale transform  $T_J$ . Riesz constants of a single-scale wavelet basis  $\Psi_j$ ,  $j < J$ , are extracted from the matrix of  $T_J$  in a straightforward way. With  $H_J^j := H_{J-1} \cdots H_j$ , one has that  $\Psi_j = \Phi_J H_J^{j+1} G_j$ , so that by orthonormality of  $\Phi_J$ ,

$$m_j = \inf_{c \neq 0} \frac{\|\Psi_j c\|_{\mathbf{L}_2}}{\|c\|_{\ell_2}} = \inf_{c \neq 0} \frac{\|\Phi_J H_J^{j+1} G_j c\|_{\mathbf{L}_2}}{\|c\|_{\ell_2}} = \sigma_{\min}(H_J^{j+1} G_j),$$

the smallest singular value of a rectangular submatrix of  $T_J$ . Analogously one finds that  $M_j$  equals the largest singular value of the same submatrix. Likewise, the complement stability constant  $\alpha_j$  equals the cosine of the angle between the column spans of two rectangular submatrices of  $T_J$ , which is easily calculated from their QR-decompositions.

## 7 Numerical Results

The previous section allows us to compute exact stability characteristics of single-scale and multiscale bases in finite-dimensional test cases.

### 7.1 Stability and Conditioning

Stability should not be seen purely as an asymptotic issue. While it is clearly desirable that the condition numbers of the multiscale transforms stay bounded as the level of the finest mesh tends to infinity, the actual magnitude of the condition numbers in practical, finite-dimensional cases is at least as important.

We compare in numerical experiments with a finite number of levels three update methods described in [18]:

- what we called the classical update, where an update stencil of width  $N$  is used to enforce orthogonality of  $\hat{\psi}_{jm}$  to  $\Pi_N$ ;
- local semiorthogonalization with fixed stencil width, which consists in orthogonalizing each wavelet  $\hat{\psi}_{jm}$  to a fixed number of neighboring scaling functions; and
- a combined update method, which stabilizes the first method by combining it with local semiorthogonalization with an adaptively chosen stencil width.

For the last method the parameter value  $\delta = .1$  was used in all examples.

Even for half MSDs on regular meshes of modest dimension, the classical update method can give unsatisfactory results. Table 1 compares for one case detailed characteristics of the bases after an update step with each of the three methods above. It is clear that for this case the classical update for five vanishing moments does not give good results at level 4. The combined update method gives better condition numbers with only moderately enlarged update support. For comparison, results are also included for local semiorthogonalization with stencil width 5, which does not yield any vanishing moments. Condition numbers for the latter two methods are close. Figure 4 shows the Gram matrices of the multiscale bases,

classical update							
level $j$	0	1	2	3	4	5	6
$\kappa(\Phi_j)$	1	1.46	1.67	2.17	1.96	1.91	1.71
$\kappa(\Psi_j)$	1	1	2.48	2.62	<b>24.0</b>	2.18	2.34
$\alpha_j$	$4 \cdot 10^{-16}$	.039	$1 \cdot 10^{-15}$	$4 \cdot 10^{-15}$	<b>.998</b>	.374	.705
width	0	0	3	5	5	5	5
local semiorthogonalization							
level $j$	0	1	2	3	4	5	6
$\kappa(\Phi_j)$	1	1.46	1.67	2.17	1.96	1.91	1.71
$\kappa(\Psi_j)$	1	1	2.48	2.62	2.35	2.19	1.71
$\alpha_j$	$2 \cdot 10^{-16}$	$4 \cdot 10^{-16}$	$3 \cdot 10^{-16}$	$9 \cdot 10^{-16}$	.043	.034	.032
width	1	2	3	5	5	5	5
combined update							
level $j$	0	1	2	3	4	5	6
$\kappa(\Phi_j)$	1	1.46	1.67	2.17	1.96	1.91	1.71
$\kappa(\Psi_j)$	1	1	2.48	2.62	2.35	2.19	1.71
$\alpha_j$	$2 \cdot 10^{-16}$	$4 \cdot 10^{-16}$	$3 \cdot 10^{-16}$	$9 \cdot 10^{-16}$	.071	.024	.034
width	1	2	3	5	5.9	6.0	5.5

Table 1: Detailed characteristics of the multiscale decompositions of order five on a regular finest-level mesh of dimension 71. Results are shown for the classical update method for five vanishing moments (condition number  $3.03 \cdot 10^2$ ), local semiorthogonalization of stencil width 5 (condition number  $3.31 \cdot 10^0$ ), and the combined update method for five vanishing moments (condition number  $3.31 \cdot 10^0$ .) This is the same example as in Figures 4 and 5.

and in Figure 5 the sparsity patterns of the update matrices are given. Note that the update stencil is enlarged mostly near the boundary, and at coarse levels where scaling functions have global support.

In this example the conditioning of the wavelet bases obtained by local semiorthogonalization and by the combined update are approximately equal. Although local semiorthogonalization performs well for multilevel meshes of moderate size, the condition numbers of the multiscale bases may keep growing as the number of levels increases. This is illustrated in Figure 7. It can be seen [18] that condition numbers of the multiscale bases are guaranteed to be uniformly bounded for *full semiorthogonalization*, where each wavelet  $\hat{\psi}_{jm}$  is orthogonalized to the whole of  $V_j$ . Local semiorthogonalization with large update stencils appears to yield a good approximation to full semiorthogonalization as far as conditioning is concerned, but it is not clear how to choose a sufficient stencil width a priori, and the resulting wavelets have no vanishing moments. Figure 8 shows condition numbers of multiscale bases constructed with the combined update method. One observes that the condition numbers depend only weakly on the number of primal vanishing moments and virtually coincide with the condition numbers of fully semiorthogonalized multiscale bases. The order  $\tilde{N}$ , however, does have a considerable influence on the conditioning. For completeness, condition numbers of the intermediate multiscale bases before the update step are plotted in Figure 6, and Table 2 repeats the numerical values for the bases from Figures 6, 7 and 8. Memory limitations in the machine on which the experiments were performed prevented us from computing the condition numbers of the largest multiscale transform matrices for full semiorthogonalization.

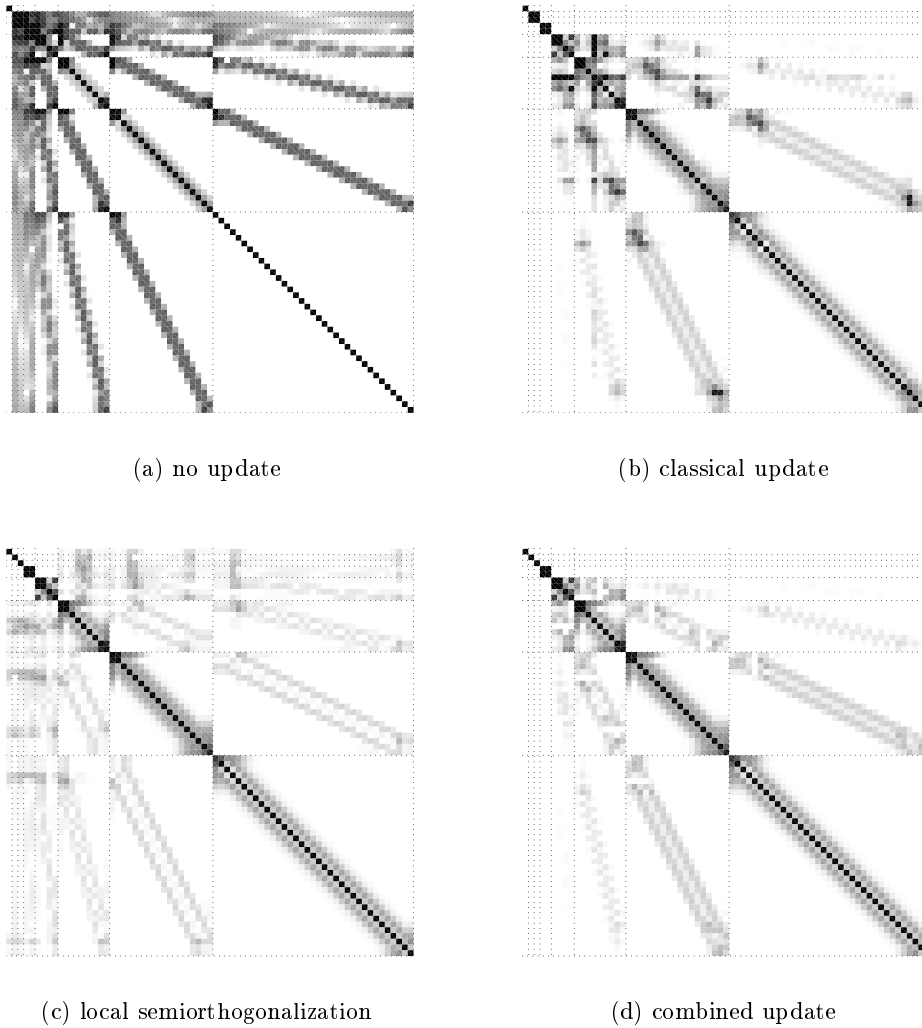
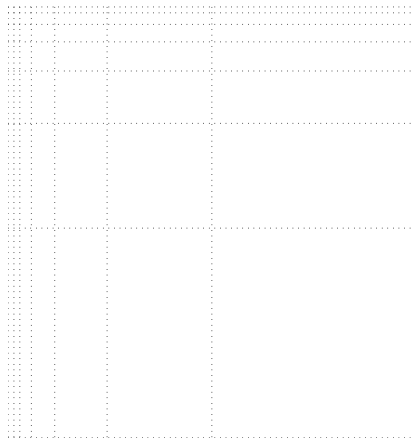
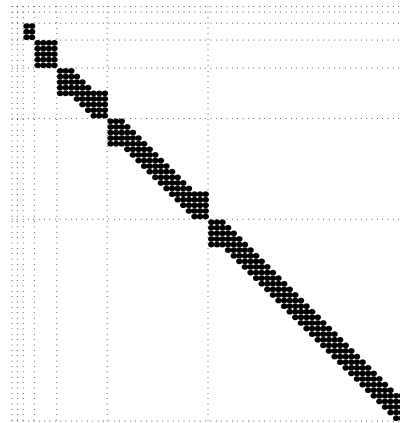


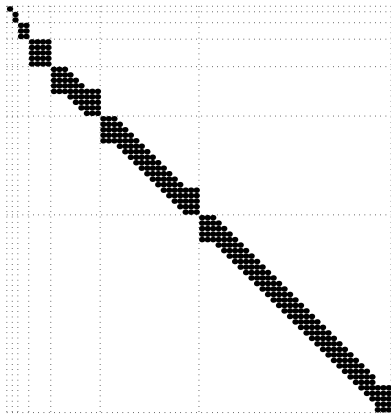
Figure 4: Magnitude of Gram matrices  $\langle \Xi_J, \Xi_J \rangle$  of multiscale bases  $\Xi_J$  of order five on a regular finest-level mesh of dimension 71, (a) before update, and (b) after a classical update step for five vanishing moments, (c) after local semiorthogonalization with stencil width 5, and (d) after a combined update step for 5 vanishing moments. Dotted lines indicate the boundaries between levels.



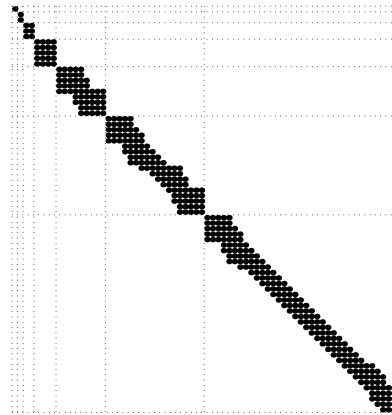
(a) no update



(b) classical update



(c) local semiorthogonalization



(d) combined update

Figure 5: Sparsity patterns of update matrices at all levels, for each of the cases in Figure 4. The update matrices are joined in a block-diagonal matrix  $\text{diag}\{U_j\}_{j=0}^{J-1}$ .

Recall that for full semiorthogonalization these matrices are dense.

The condition numbers of multiscale transforms from the stabilized two-step construction also compare favorably to those from the construction in [8], where the authors report condition numbers in excess of  $10^1$ ,  $10^3$ ,  $10^6$  and  $10^{11}$  for  $\tilde{N} = N = 3, 5, 7$ , and  $9$ , respectively.

## 7.2 Influence of the Irregularity of the Mesh

Figure 9 shows the largest and smallest computed condition numbers of multiscale bases of order three on pseudo-random irregular meshes of various dimensions as a function of the homogeneity constant  $\gamma$  from (4.4). The brute-force approach was to generate an irregular multilevel mesh, compute the condition number of the multiscale basis on this mesh and keep only the envelope of all results. For the combined update method, the presence of an upper bound on the condition number as a function of  $\gamma$  is apparent, but we do not have a closed-form expression for an upper bound available. One observes that the classical update method can give badly conditioned multiscale bases already on moderately irregular meshes. Condition numbers for full semiorthogonalization again almost coincide with those for the combined update method, and are not shown.

Figure 10 repeats the experiment for order seven. In all numerical experiments with average-interpolation of orders higher than three on homogeneous irregular meshes we observed convergence, although no general theoretical result is available to our knowledge.

It should be noted that in our simple coarsening procedure  $\gamma$  is not bounded uniformly over all bounded regular finest-level meshes. The algorithm transforms a regular finest-level mesh into an irregular multilevel mesh the homogeneity constant of which is unbounded when the dimension of the finest level is allowed to grow. The worst case for regular meshes are those of dimension  $2^k(2^n + 1)$ , giving rise to a value for  $\gamma$  of  $2^n$  and to single-scale bases with condition numbers that grow as  $2^{n/2}$ . The effect is illustrated in Figure 11. Alternative coarsening strategies may circumvent this problem but remain to be investigated.

## 8 Conclusion

We have applied the results of [18] to average-interpolating biorthogonal multiresolutions on irregular meshes on the interval. For stability it is required that the irregular multilevel mesh is homogeneous. The conditioning of the bases depends on the homogeneity constant of the multilevel mesh.

The desired stability properties of the prediction step are seen to follow from convergence properties of average-interpolating subdivision schemes, which produce scaling functions that are biorthogonal to known dual bases of normalized characteristic functions. If the subdivision scheme converges and gives uniformly bounded scaling functions, a series of stability properties follow. Firstly, the bases of primal scaling functions are uniformly stable. Secondly, the lifting mechanism identifies uniformly stable primal and dual wavelet bases for the complement spaces in the new pair of biorthogonal MSDs. Uniform complement stability is guaranteed. In the update step we use the stabilized update method discussed in [18]. The scaling functions and wavelets on both the primal and the dual side are local.

Numerical experiments show that the classical update is unstable on irregular meshes, while the stabilized update method produces multiscale bases with approximately the same condition numbers as full semiorthogonalization using only slightly larger update stencils than the classical update.

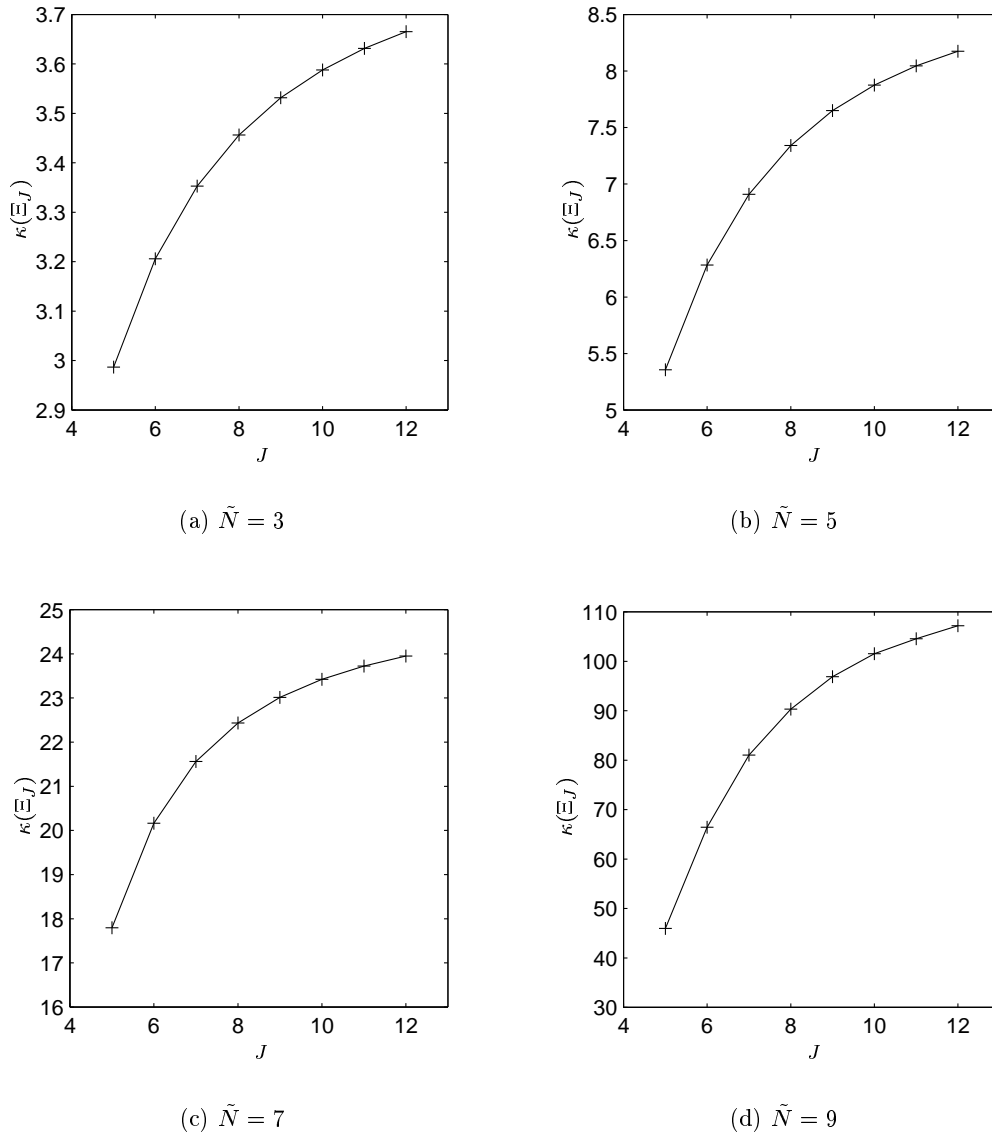


Figure 6: Condition numbers of multiscale bases of order  $\tilde{N}$  without update, on regular multilevel meshes for an increasing number of levels  $J$ . The finest-level mesh is of dimension  $2^J$ .

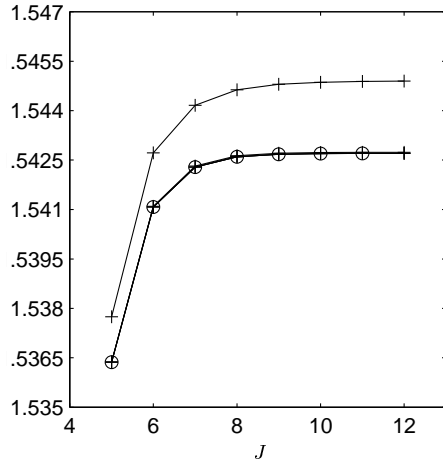
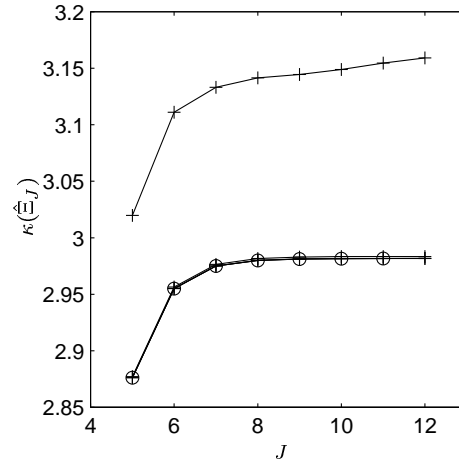
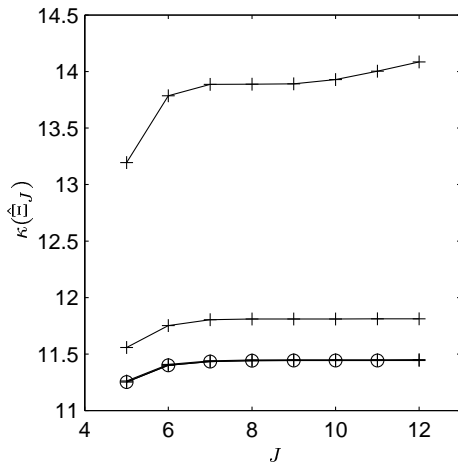
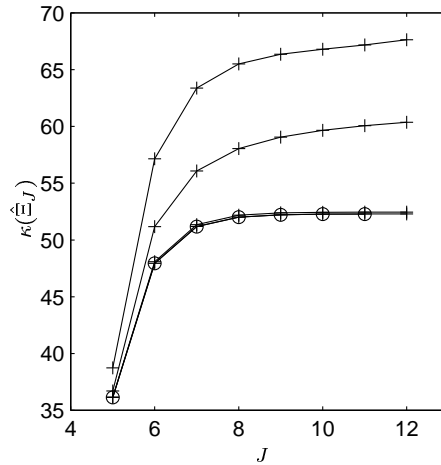
(a)  $\tilde{N} = 3$ , width = 3, 5, 7, 9,  $\infty$ (b)  $\tilde{N} = 5$ , width = 3, 5, 7, 9,  $\infty$ (c)  $\tilde{N} = 7$ , width = 3, 5, 7, 9,  $\infty$ (d)  $\tilde{N} = 9$ , width = 3, 5, 7, 9,  $\infty$ 

Figure 7: Condition numbers of multiscale bases obtained by local semiorthogonalization and by full semiorthogonalization, on regular multilevel meshes for an increasing number of levels  $J$ . Results are shown for several choices of the order  $\tilde{N}$  and several widths of the update stencil. Full semiorthogonalization corresponds to a stencil width of  $\infty$  and is indicated in the graphs by ‘o’ markers. Within each subplot, condition numbers decrease when the stencil is enlarged.

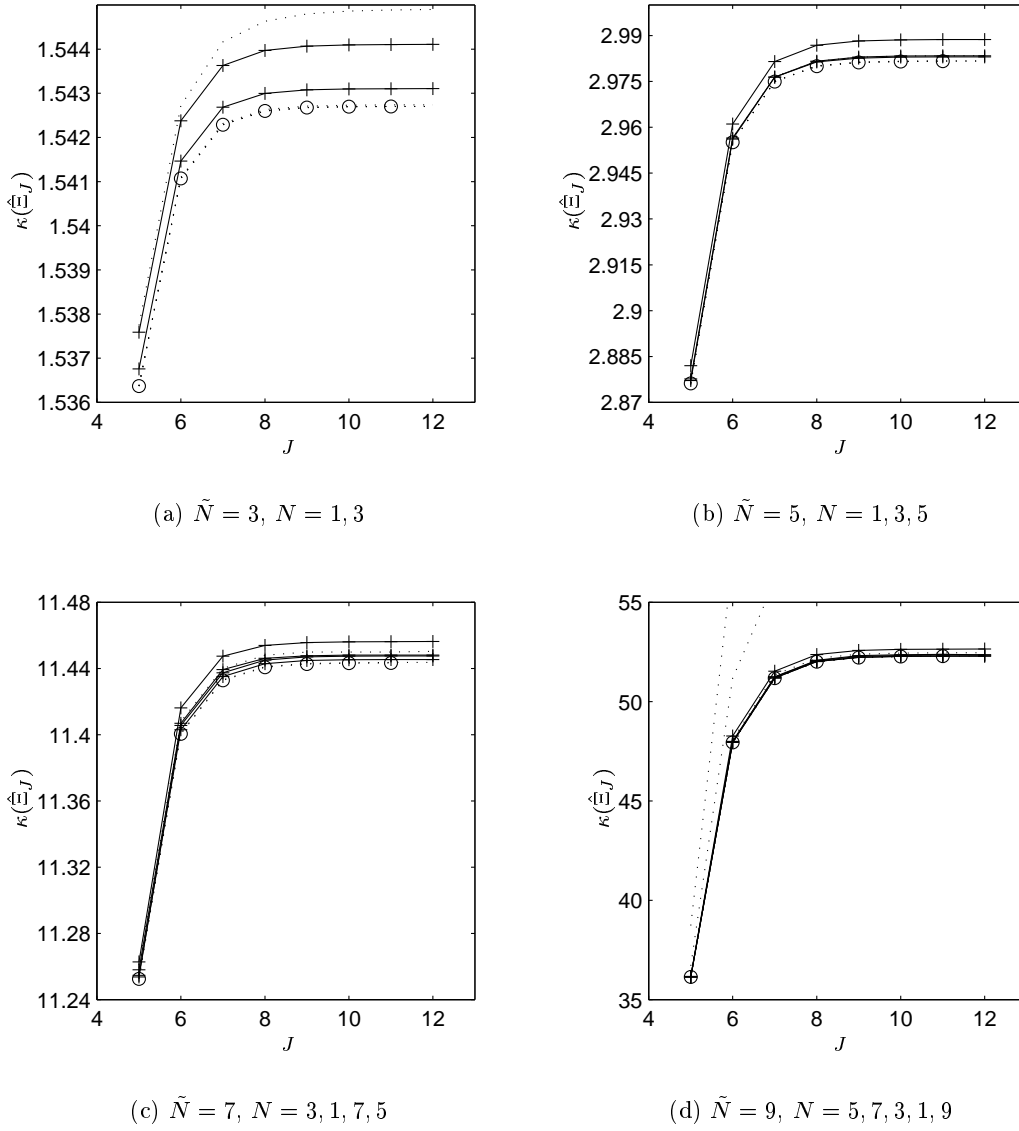


Figure 8: Condition numbers of multiscale bases obtained by the combined update method, on regular multilevel meshes for an increasing number of levels  $J$ . For comparison, the values from Figure 7 are repeated in dotted line.

no update									
$\tilde{N}$	$N$	$J$							
		5	6	7	8	9	10	11	12
3	1	2.9868	3.2061	3.3531	3.4563	3.5316	3.5880	3.6314	3.6654
5	1	5.3560	6.2838	6.9086	7.3417	7.6503	7.8764	8.0460	8.1760
7	1	17.794	20.162	21.564	22.432	23.012	23.422	23.722	23.949
9	1	45.964	66.416	81.045	90.331	96.867	101.53	104.55	107.19
local semiorthogonalization									
$\tilde{N}$	width	$J$							
		5	6	7	8	9	10	11	12
3	3	1.5377	1.5427	1.5442	1.5446	1.5448	1.5449	1.5449	1.5449
3	5	1.5364	1.5411	1.5423	1.5426	1.5427	1.5427	1.5427	1.5427
3	7	1.5364	1.5411	1.5423	1.5426	1.5427	1.5427	1.5427	1.5427
3	9	1.5364	1.5411	1.5423	1.5426	1.5427	1.5427	1.5427	1.5427
5	3	3.0198	3.1111	3.1332	3.1415	3.1445	3.1489	3.1546	3.1591
5	5	2.8771	2.9564	2.9765	2.9816	2.9829	2.9833	2.9834	2.9834
5	7	2.8762	2.9551	2.9751	2.9801	2.9813	2.9816	2.9817	2.9817
5	9	2.8762	2.9551	2.9750	2.9800	2.9812	2.9815	2.9816	2.9816
7	3	13.195	13.786	13.887	13.889	13.891	13.929	14.004	14.085
7	5	11.559	11.752	11.803	11.810	11.810	11.811	11.811	11.812
7	7	11.261	11.408	11.440	11.448	11.450	11.450	11.450	11.450
7	9	11.253	11.401	11.433	11.441	11.443	11.444	11.444	11.444
9	3	38.733	57.156	63.378	65.511	66.361	66.800	67.172	67.636
9	5	36.704	51.177	56.084	58.057	59.059	59.659	60.067	60.372
9	7	36.163	48.088	51.348	52.180	52.390	52.443	52.457	52.460
9	9	36.141	47.944	51.185	52.014	52.222	52.274	52.288	52.291

Table 2: Condition numbers of multiscale bases on regular multilevel meshes for an increasing number of levels  $J$ . A dagger ‘†’ indicates a missing value.

full semiorthogonalization										
$\tilde{N}$	$N$	$J$								
		5	6	7	8	9	10	11	12	
3	3	1.5364	1.5411	1.5423	1.5426	1.5427	1.5427	1.5427	1.5427	†
5	5	2.8762	2.9551	2.9750	2.9800	2.9812	2.9815	2.9816	2.9816	†
7	7	11.253	11.400	11.433	11.441	11.443	11.443	11.443	11.443	†
9	9	36.141	47.942	51.183	52.012	52.221	52.273	52.286	52.286	†

combined update										
$\tilde{N}$	$N$	$J$								
		5	6	7	8	9	10	11	12	
3	1	1.5376	1.5424	1.5436	1.5440	1.5441	1.5441	1.5441	1.5441	1.5441
3	3	1.5368	1.5415	1.5427	1.5430	1.5431	1.5431	1.5431	1.5431	1.5431
5	1	2.8820	2.9611	2.9815	2.9868	2.9882	2.9886	2.9887	2.9887	2.9887
5	3	2.8772	2.9561	2.9764	2.9816	2.9830	2.9833	2.9834	2.9834	2.9834
5	5	2.8777	2.9565	2.9764	2.9814	2.9826	2.9829	2.9830	2.9830	2.9830
7	1	11.258	11.407	11.439	11.446	11.448	11.448	11.448	11.448	11.448
7	3	11.263	11.416	11.447	11.454	11.456	11.456	11.456	11.456	11.456
7	5	11.255	11.403	11.435	11.443	11.445	11.445	11.445	11.445	11.445
7	7	11.254	11.406	11.437	11.445	11.447	11.447	11.448	11.448	11.448
9	1	36.142	47.946	51.188	52.017	52.226	52.278	52.291	52.294	52.294
9	3	36.144	47.979	51.233	52.064	52.273	52.325	52.338	52.341	52.341
9	5	36.168	48.269	51.532	52.367	52.577	52.630	52.643	52.646	52.646
9	7	36.147	48.003	51.252	52.082	52.291	52.344	52.357	52.360	52.360
9	9	36.144	47.944	51.186	52.015	52.223	52.275	52.288	52.291	52.291

Table 2 (continued)

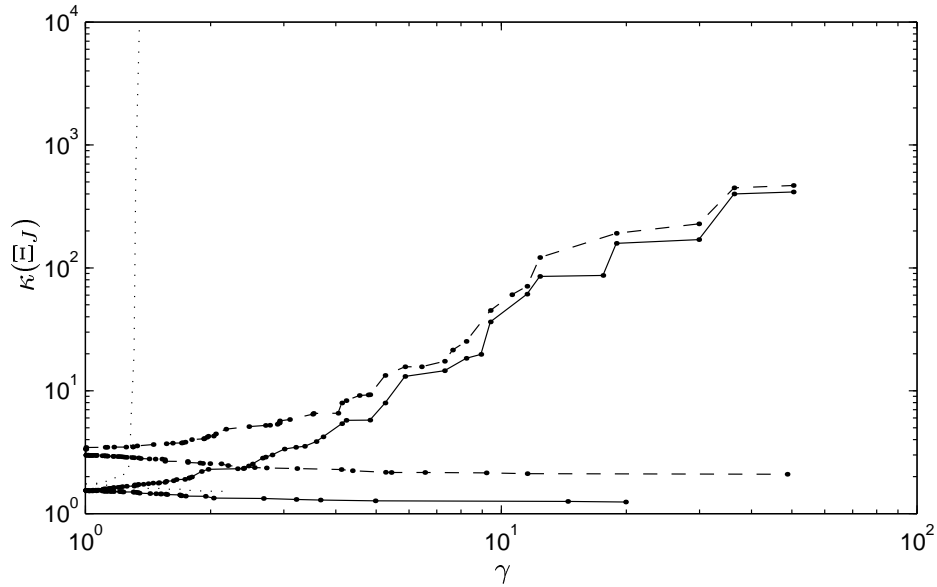


Figure 9: Computed envelopes of condition numbers of multiscale bases of order three on pseudo-random irregular meshes of various dimensions. The dashed line shows the condition numbers of the bases before the final update step. The solid line shows the condition numbers for the same meshes after use of the combined update method to obtain three vanishing moments. The dotted line gives the results for the classical update method.

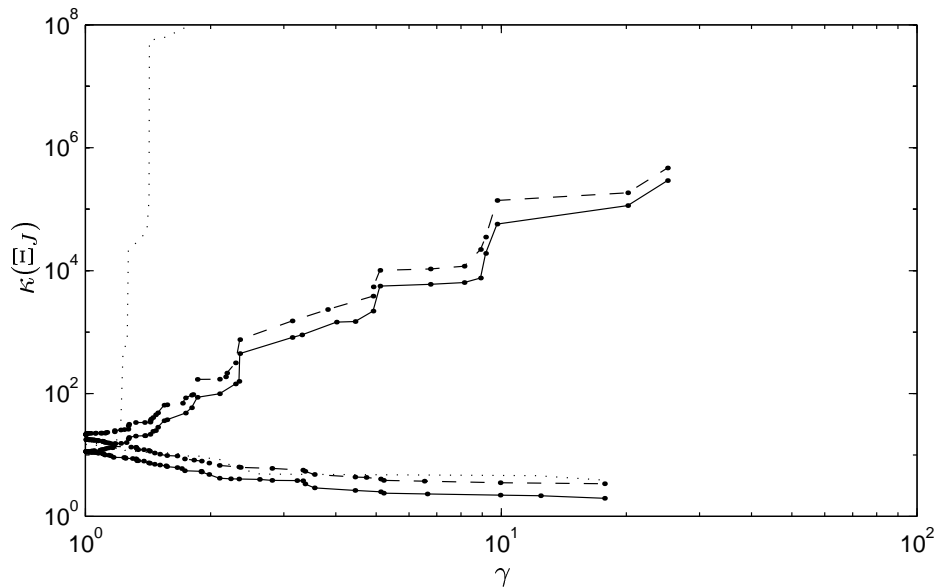


Figure 10: Computed envelopes of condition numbers of multiscale bases of order seven, repeating the experiment of Figure 9.

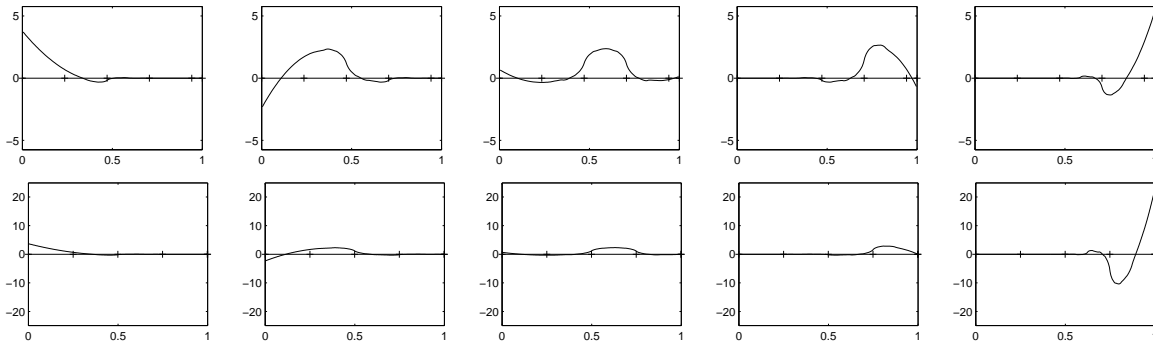


Figure 11: Single-scale bases  $\Phi_3$  of order three on a regular mesh of dimension  $2^k(2^n + 1)$ , for  $n = 4$  (top row) and  $n = 9$  (bottom row). In the latter mesh, the rightmost interval is invisibly small. The norm of the rightmost scaling function grows as  $2^{n/2}$ .

## Acknowledgments

This paper presents research results of the Belgian Program on Interuniversity Poles of Attraction, initiated by the Belgian State, Prime Minister's Office for Science, Technology and Culture. The scientific responsibility rests with the authors.

The first author was funded as a Research Assistant of the Fund for Scientific Research – Flanders, Belgium (F.W.O.).

## References

- [1] J. Carnicer, W. Dahmen, and J. Peña. Local decomposition of refinable spaces and wavelets. *Appl. Comput. Harmon. Anal.*, 3:127–153, 1996.
- [2] A. S. Cavaretta, W. Dahmen, and C. A. Micchelli. *Stationary subdivision*. Number 453 in Memoirs of the Amer. Math. Soc. Amer. Math. Soc., 1991.
- [3] C. K. Chui. *An Introduction to Wavelets*, volume 1 of *Wavelet Analysis and Its Applications*. Academic Press, San Diego, 1992.
- [4] A. Cohen, I. Daubechies, and J.-C. Feauveau. Biorthogonal bases of compactly supported wavelets. *Comm. Pure Appl. Math.*, 55:485–560, 1992.
- [5] A. Cohen, I. Daubechies, and P. Vial. Wavelets on the interval and fast wavelet transforms. *Appl. Comput. Harmon. Anal.*, 1:54–81, 1994.
- [6] W. Dahmen. Stability of multiscale transformations. *J. Fourier Anal. Appl.*, 4:341–362, 1996.
- [7] W. Dahmen. Wavelet and multiscale methods for operator equations. In *Acta Numerica*, volume 6, pages 55–228. Cambridge Univ. Press, Cambridge, 1997.
- [8] W. Dahmen, A. Kunoth, and K. Urban. Biorthogonal spline-wavelets on the interval: Stability and moment conditions. *Appl. Comput. Harmon. Anal.*, 6:132–196, 1999.

- [9] W. Dahmen and R. P. Stevenson. Element-by-element construction of wavelets satisfying stability and moment conditions. *SIAM J. Numer. Anal.*, 37(1):319–352, 1999.
- [10] I. Daubechies, I. Guskov, and W. Sweldens. Commutation for irregular subdivision. Preprint, Bell Laboratories, Lucent Technologies, 1998.
- [11] I. Daubechies, I. Guskov, and W. Sweldens. Regularity of irregular subdivision. *Constr. Approx.*, 15(3):381–426, 1999.
- [12] I. Daubechies and W. Sweldens. Factoring wavelet transforms into lifting steps. *J. Fourier Anal. Appl.*, 4(3), 1999.
- [13] G. Deslauriers and S. Dubuc. Interpolation dyadique. In *Fractales, Dimensions Non-entières et Applications*, pages 44–55. Masson, Paris, 1987.
- [14] D. L. Donoho. Smooth wavelet decompositions with blocky coefficient kernels. In [17], pages 259–308.
- [15] S. Dubuc. Interpolation through an iterative scheme. *J. Math. Anal. and Appl.*, 114:185–204, 1986.
- [16] N. Dyn. Subdivision schemes in Computer Aided Geometric Design. In W. A. Light, editor, *Wavelets, Subdivision Algorithms, and Radial Basis Functions*, volume II of *Advances in Numerical Analysis*, chapter 2, pages 36–104. Oxford UP, Oxford, UK, 1992.
- [17] L. L. Schumaker and G. Webb, editors. *Recent Advances in Wavelet Analysis*. Academic Press, New York, 1993.
- [18] J. Simoens and S. Vandewalle. On the stability of wavelet bases in the lifting scheme. Report TW306, Dept. of Computer Science, Katholieke Universiteit Leuven, Belgium, Apr. 2000.
- [19] R. P. Stevenson. Piecewise linear (pre-)wavelets on non-uniform meshes. In W. Hackbusch and G. Wittum, editors, *Multigrid Methods V. Proceedings of the Fifth European Multigrid Conference, Stuttgart, October 1996*, volume 3 of *Lecture Notes in Computational Science and Engineering*, pages 306–319, Heidelberg, 1998. Springer-Verlag.
- [20] R. P. Stevenson. Stable three-point wavelet bases on general meshes. *Numer. Math.*, 80:131–158, 1998.
- [21] W. Sweldens. The lifting scheme: A construction of second generation wavelets. *SIAM J. Math. Anal.*, 29(2):511–546, 1997.
- [22] H. Yserentant. On the multi-level splitting of finite element spaces. *Numer. Math.*, 49:379–412, 1986.